Cosmology and the Large Scale Structure of the Universe

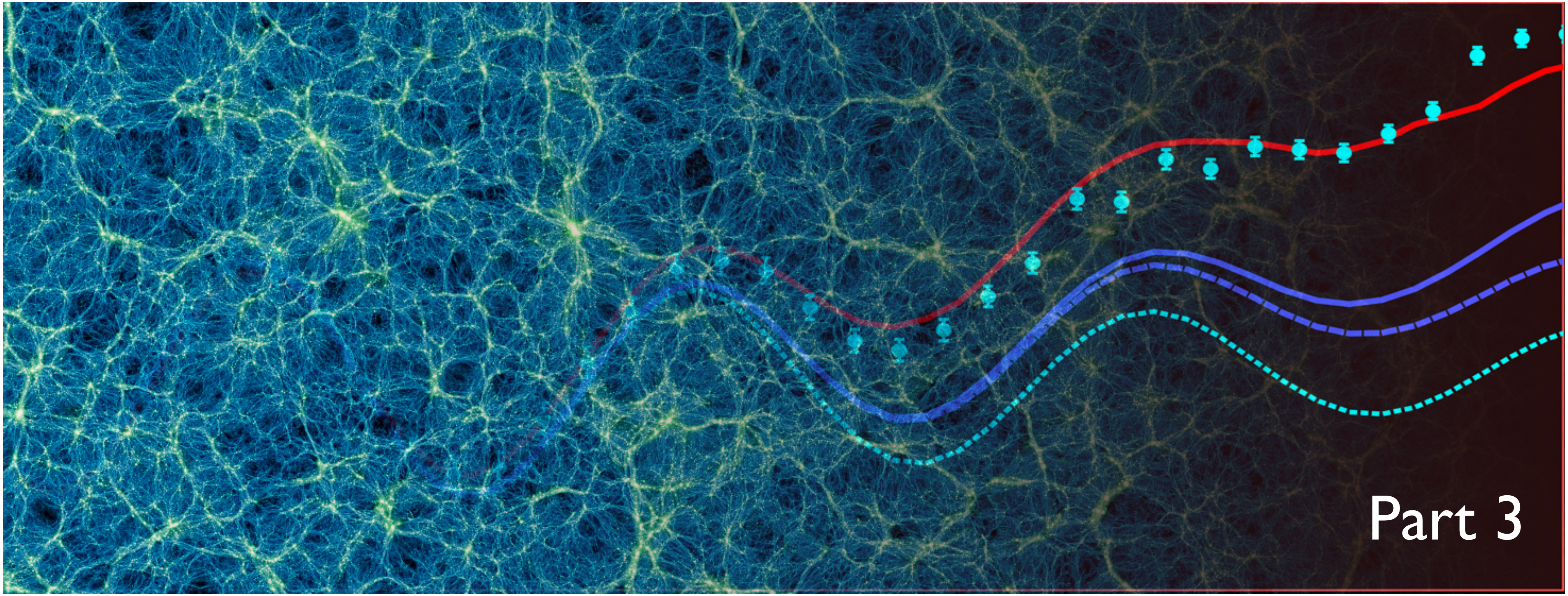

Emiliano Sefusatti
Astronomical Observatory of Brera
National Institute for Astrophysics

Recap

Goal:
predict the correlation functions describing the statistical properties of the Large-Scale Structure, in particular of the galaxy distribution

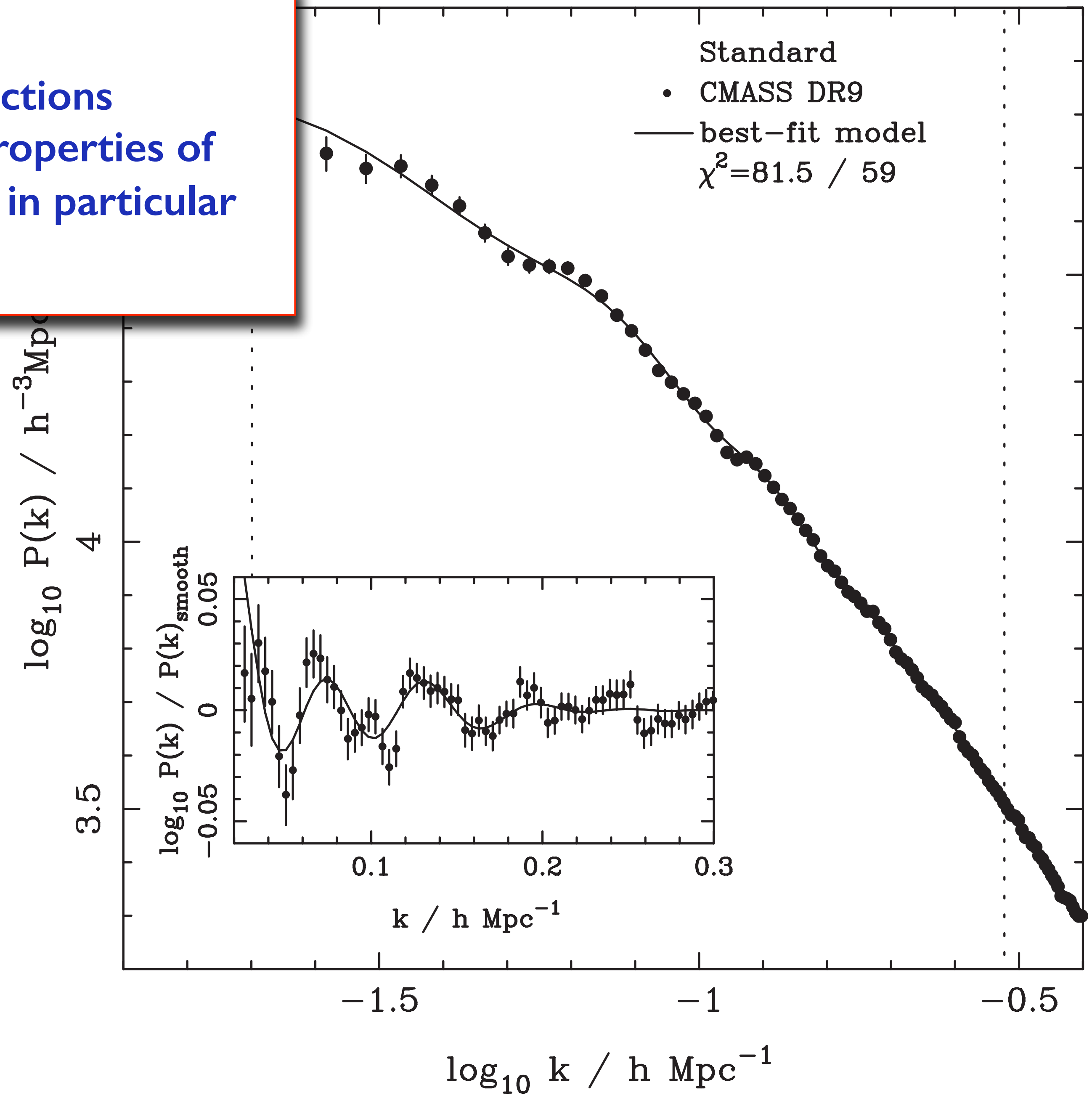

Recap

Goal:
predict the correlation functions describing the statistical properties of the Large-Scale Structure, in particular of the galaxy distribution

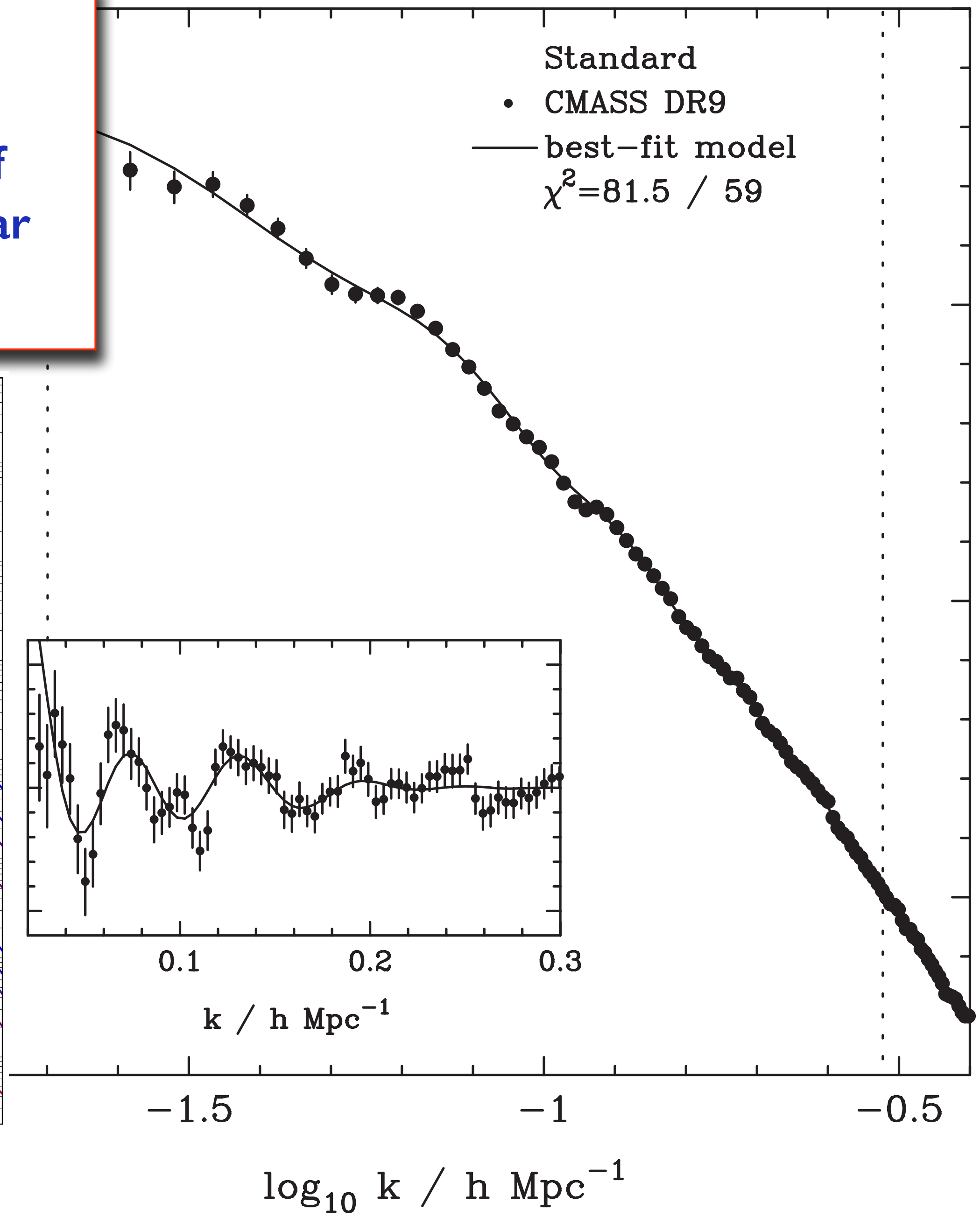

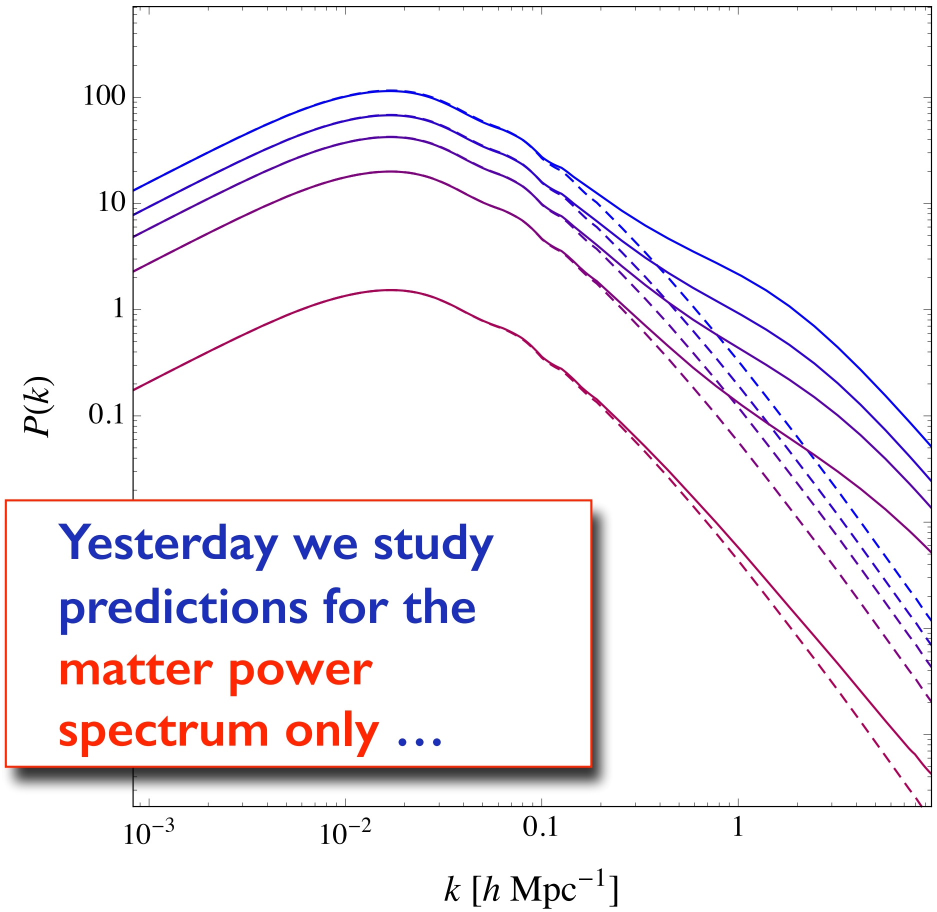

Yesterday we study predictions for the matter power spectrum only …

Today

The galaxy power spectrum

Baryonic Acoustic Oscillations

Redshift Space Distortions

The effect of neutrino mass

Galaxies

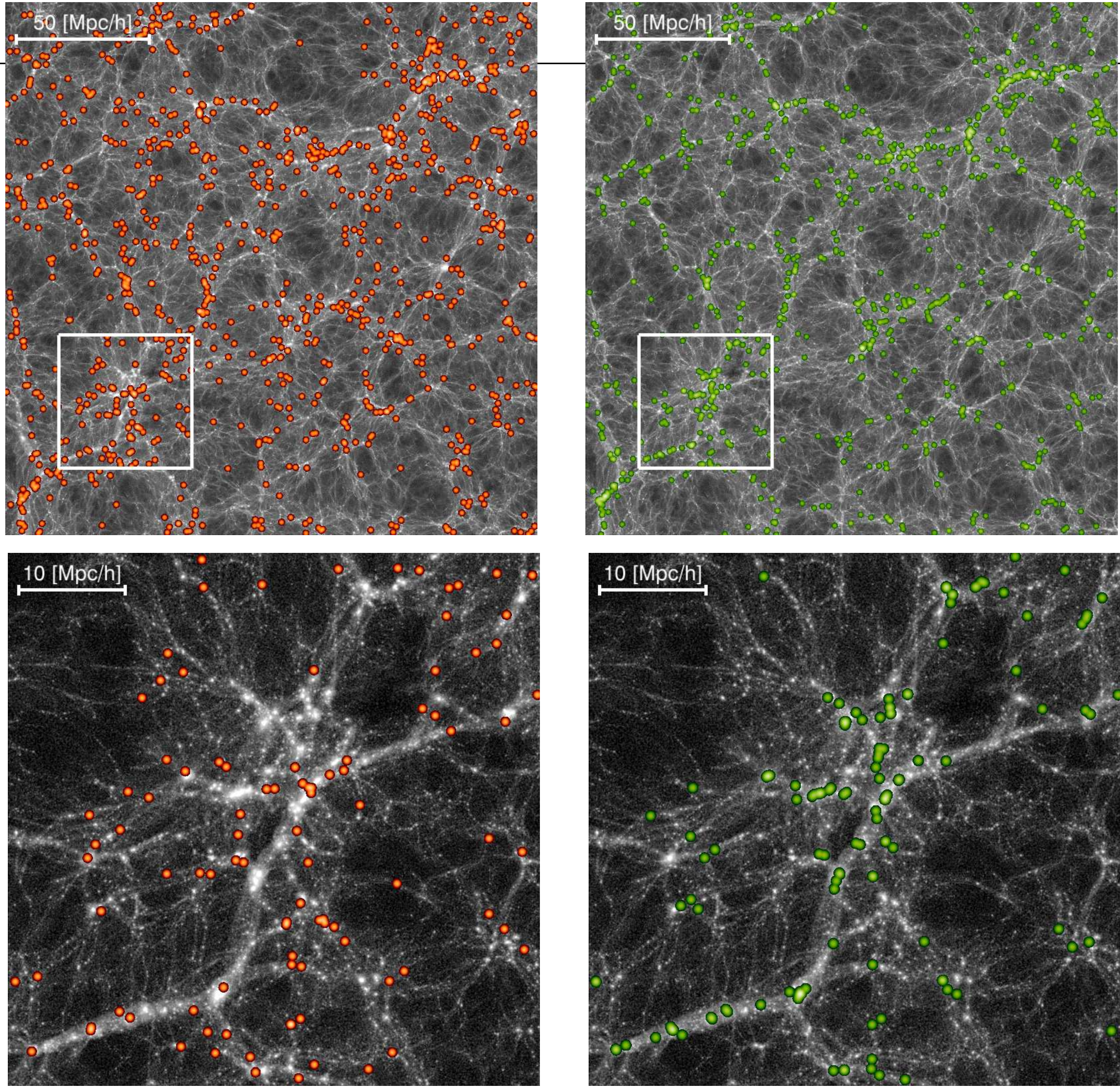

[Orsi *et al.* (2009)]

Local galaxy bias

A very simple assumption ...

local galaxy bias

$$\delta_g(x) \equiv \frac{n_g(x) - \bar{n}_g}{\bar{n}_g} = f\left[\delta(x)\right]$$

If galaxies form in regions of large dark matter density, I can at least expect a direct dependence of the **galaxy overdensity** on the **matter overdensity**

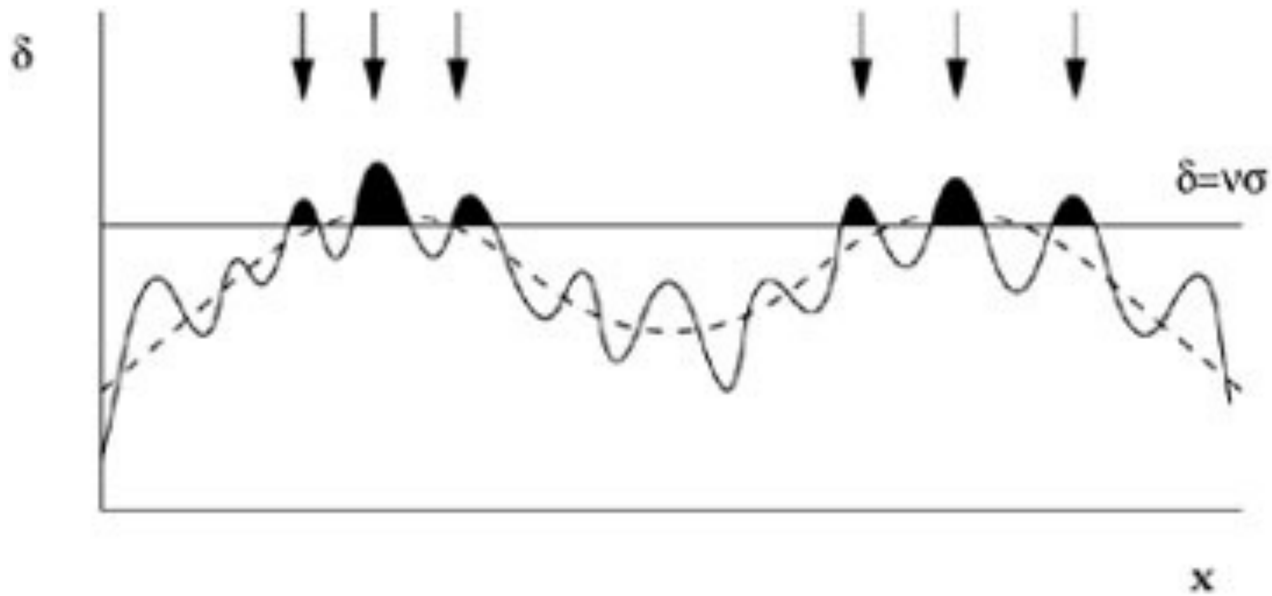

Local galaxy bias

A very simple assumption …

local galaxy bias

$$\delta_g(x) \equiv \frac{n_g(x) - \bar{n}_g}{\bar{n}_g} = f\,[\delta(x)]$$

At large scales, we can expand it in a Taylor series

$$\delta_g(x) = b\,\delta(x) + \frac{1}{2}\,b_2\,\delta^2(x) + \ldots$$

linear bias nonlinear bias corrections

$$\langle \delta_g \delta_g \rangle = b^2\,\langle \delta\delta \rangle$$

$$\xi_g(x) \simeq b^2 \xi(x)$$

$$P_g(k) \simeq b^2 P(k)$$

At *large* scales, we expect a very **simple, linear relation between galaxy and matter correlation functions**

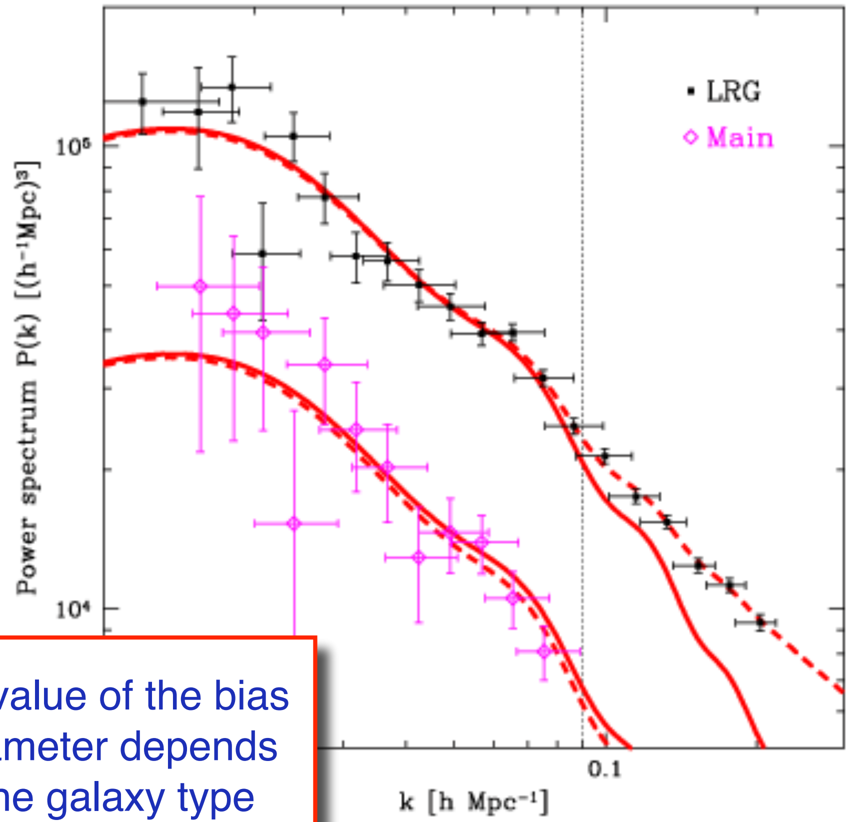

the value of the bias parameter depends on the galaxy type

Non-linear bias *and* non-linear gravitational instability

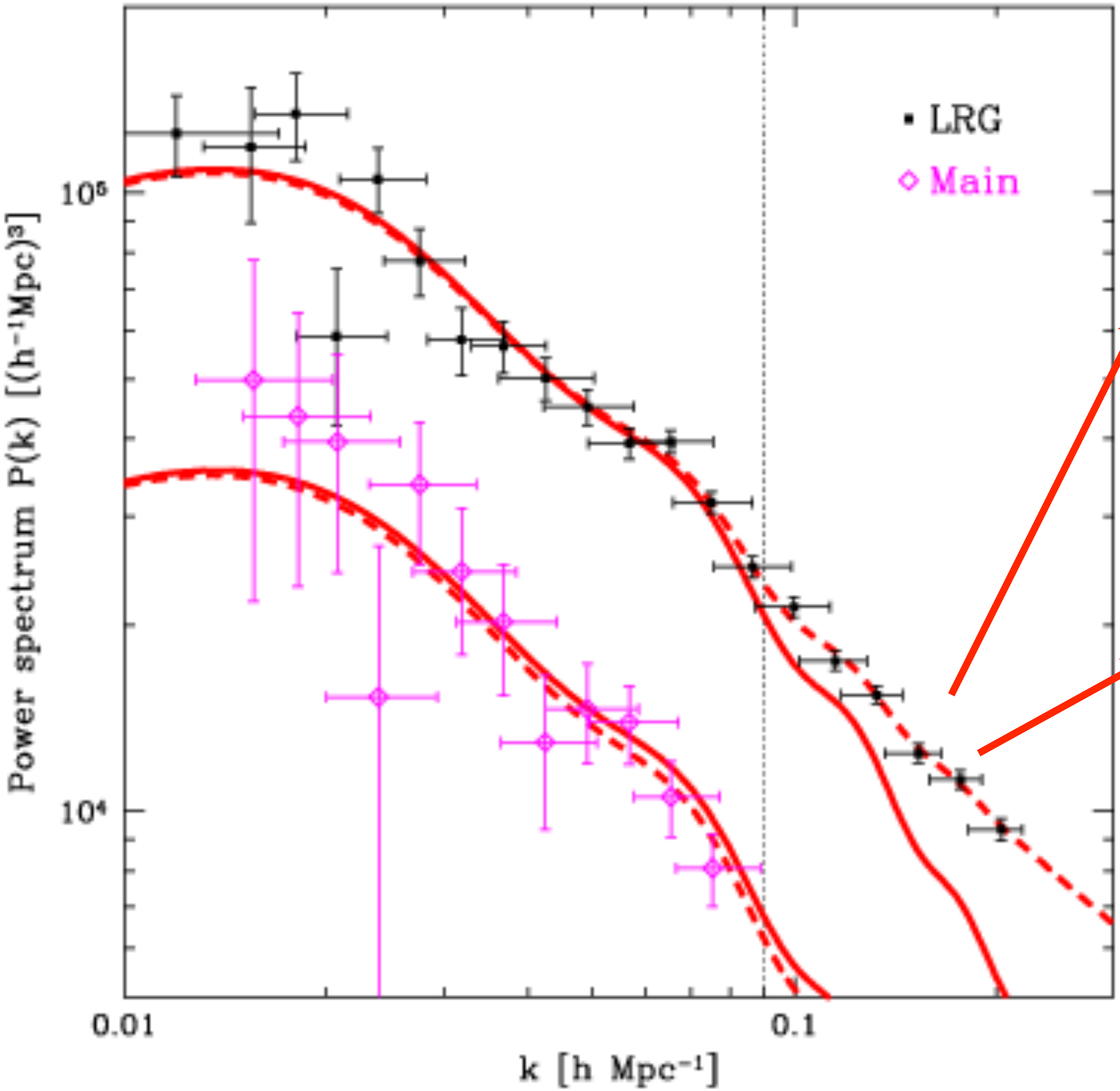

at small scales, non-linear bias is degenerate with non-linear corrections to the matter power spectrum!

at small scales we also have better statistics (smaller error bars)

Baryonic Acoustic Oscillations
in the galaxy distribution

Baryonic Acoustic Oscillations

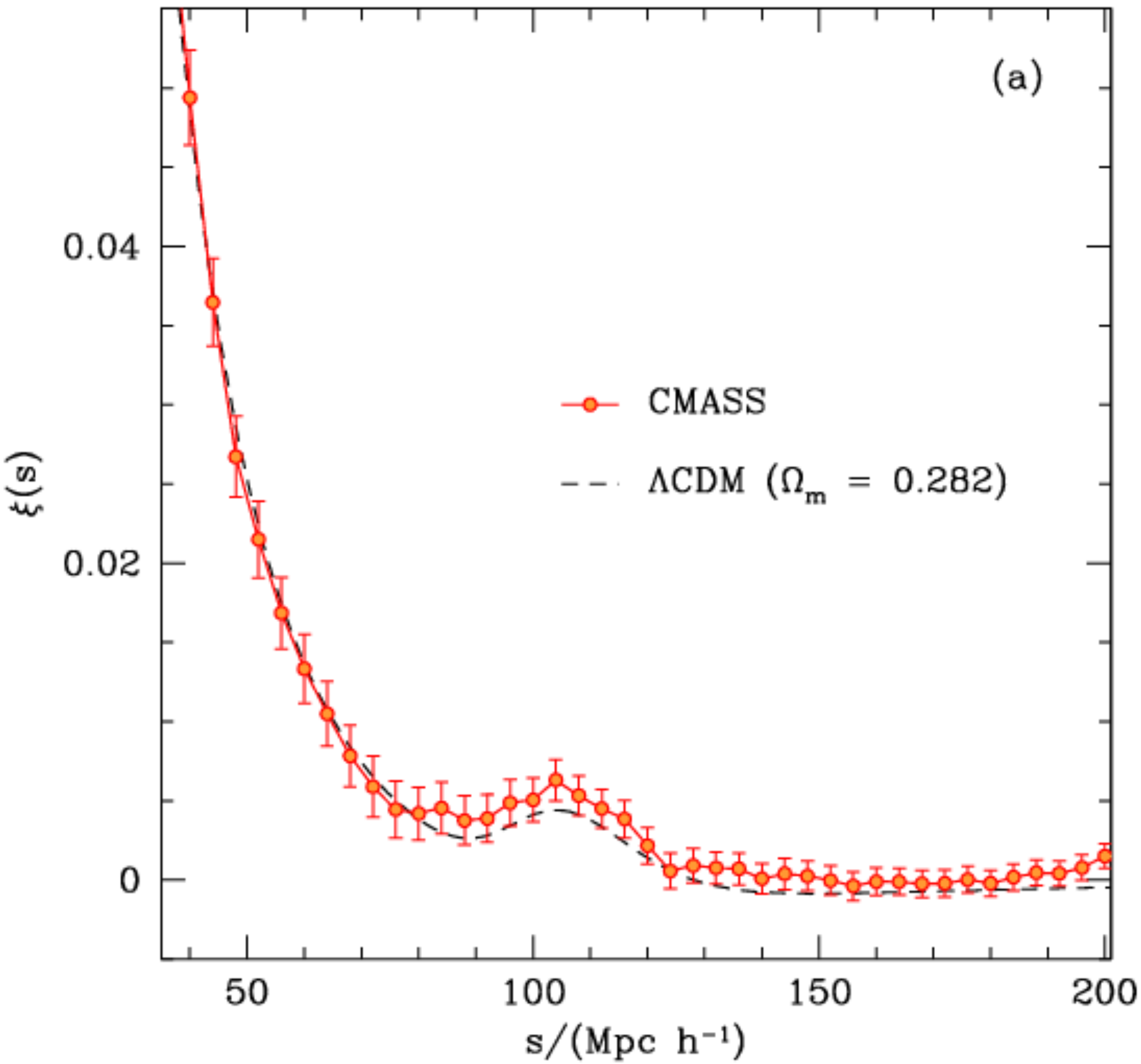

Baryonic Acoustic Oscillations

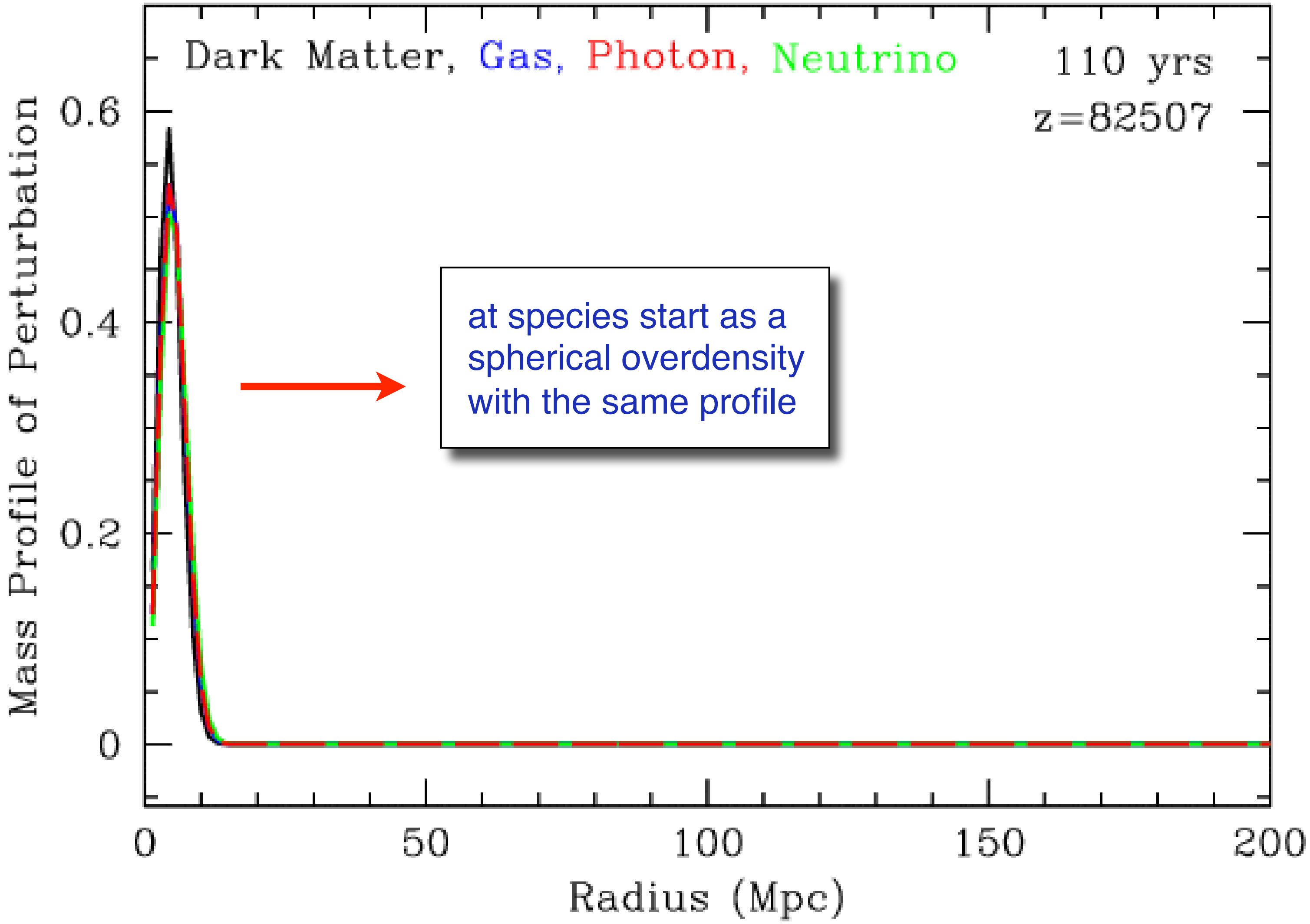

Radiation domination

[credit: Daniel Eisenstein]

Baryonic Acoustic Oscillations

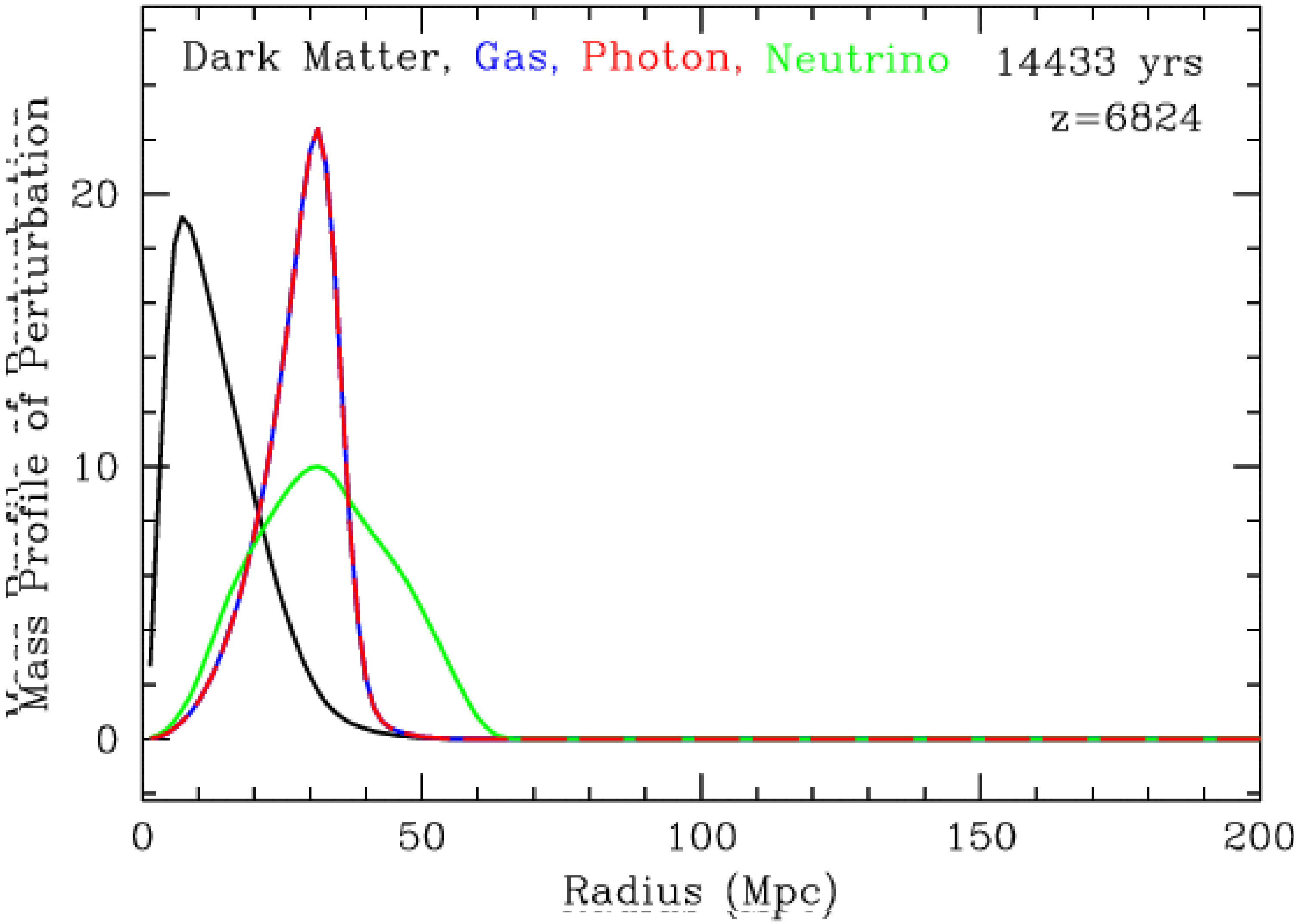

Matter domination

[credit: Daniel Eisenstein]

Baryonic Acoustic Oscillations

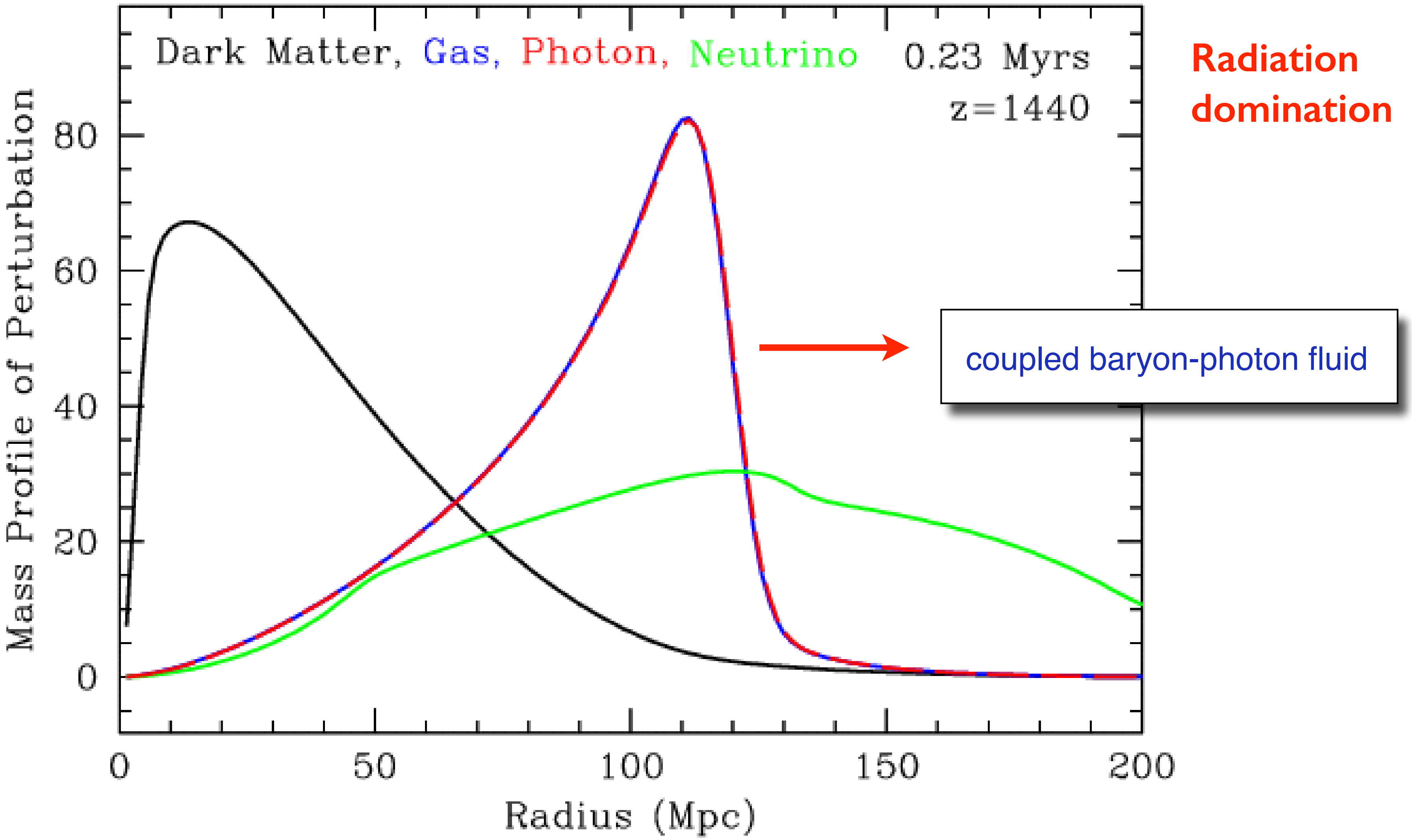

Radiation domination

[credit: Daniel Eisenstein]

Baryonic Acoustic Oscillations

Photon decoupling: the density is low enough that photon free-stream away …

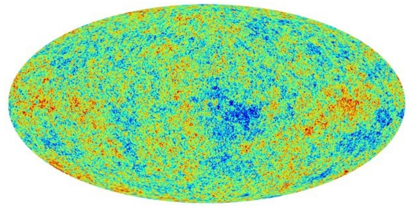

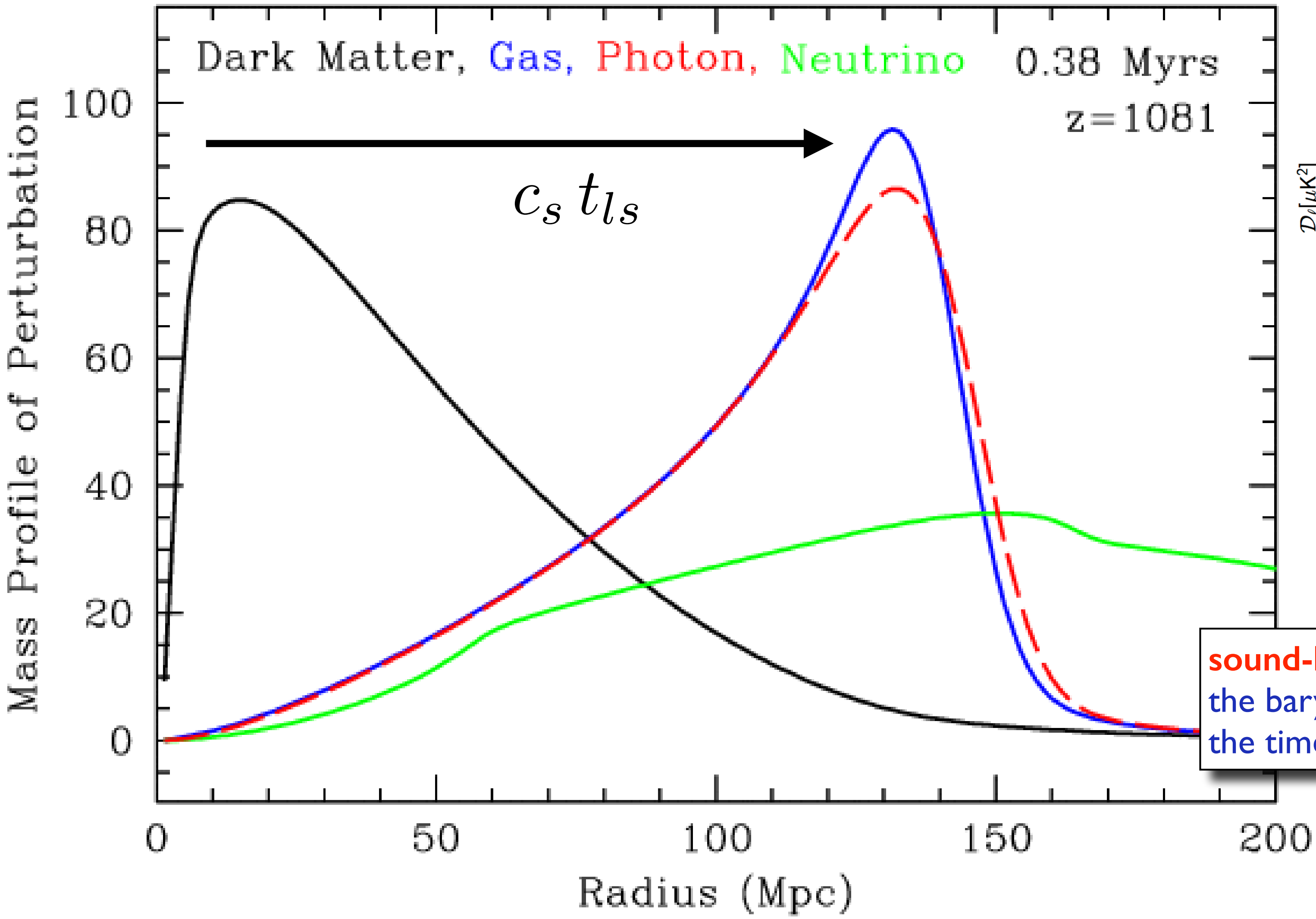

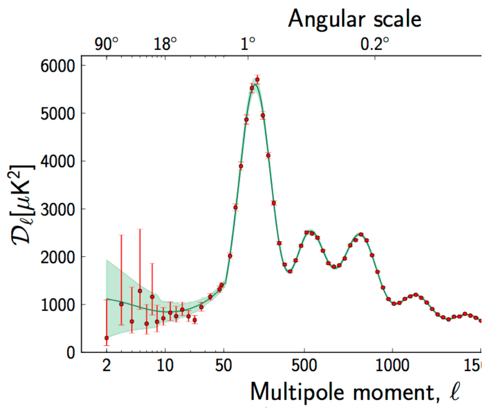

$$c_s\, t_{ls}\, k = \pi$$

sound-horizon: sound-speed of the baryon-photon fluid *times* the time of last scattering

[credit: Daniel Eisenstein]

Baryonic Acoustic Oscillations

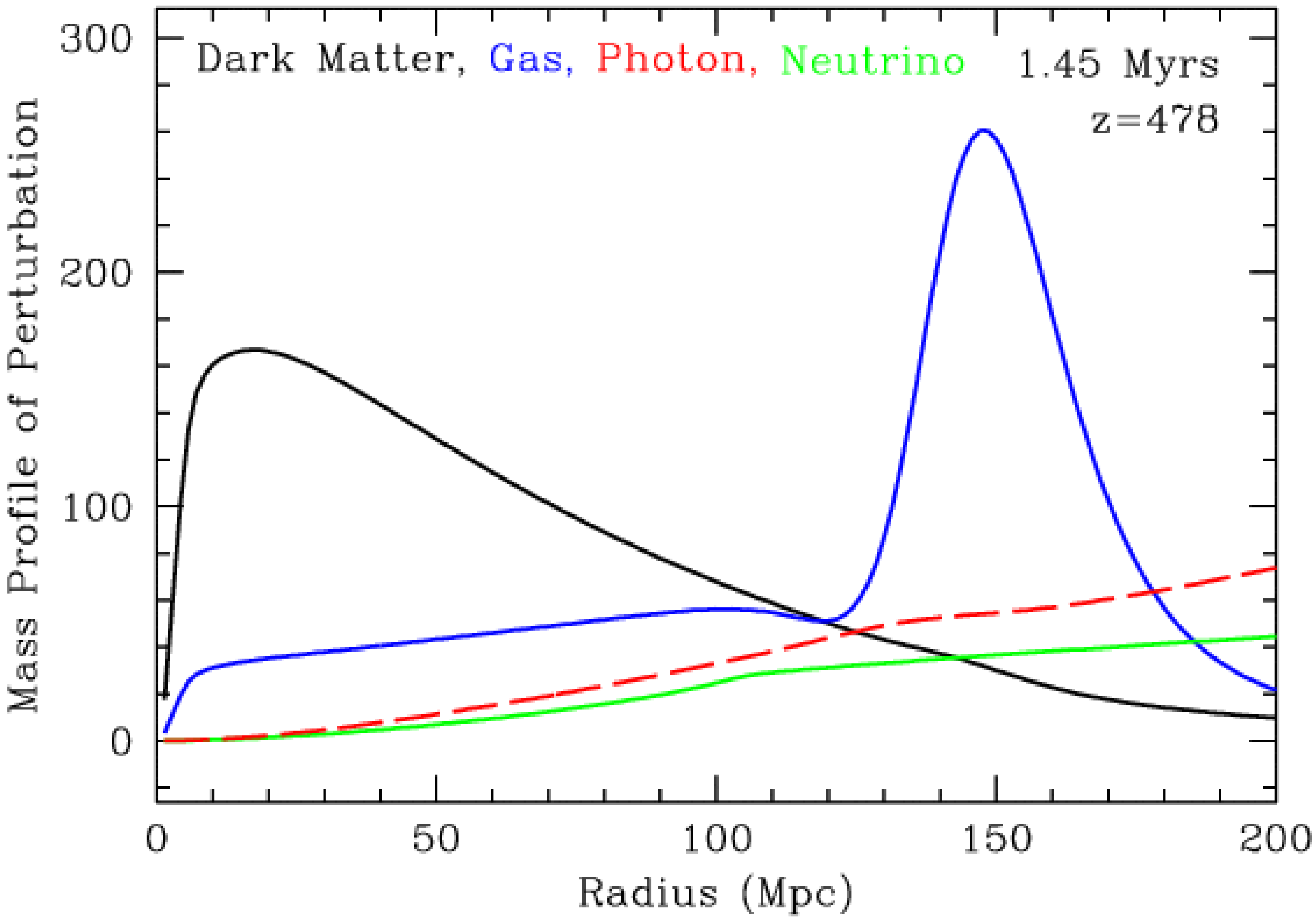

[credit: Daniel Eisenstein]

Baryonic Acoustic Oscillations

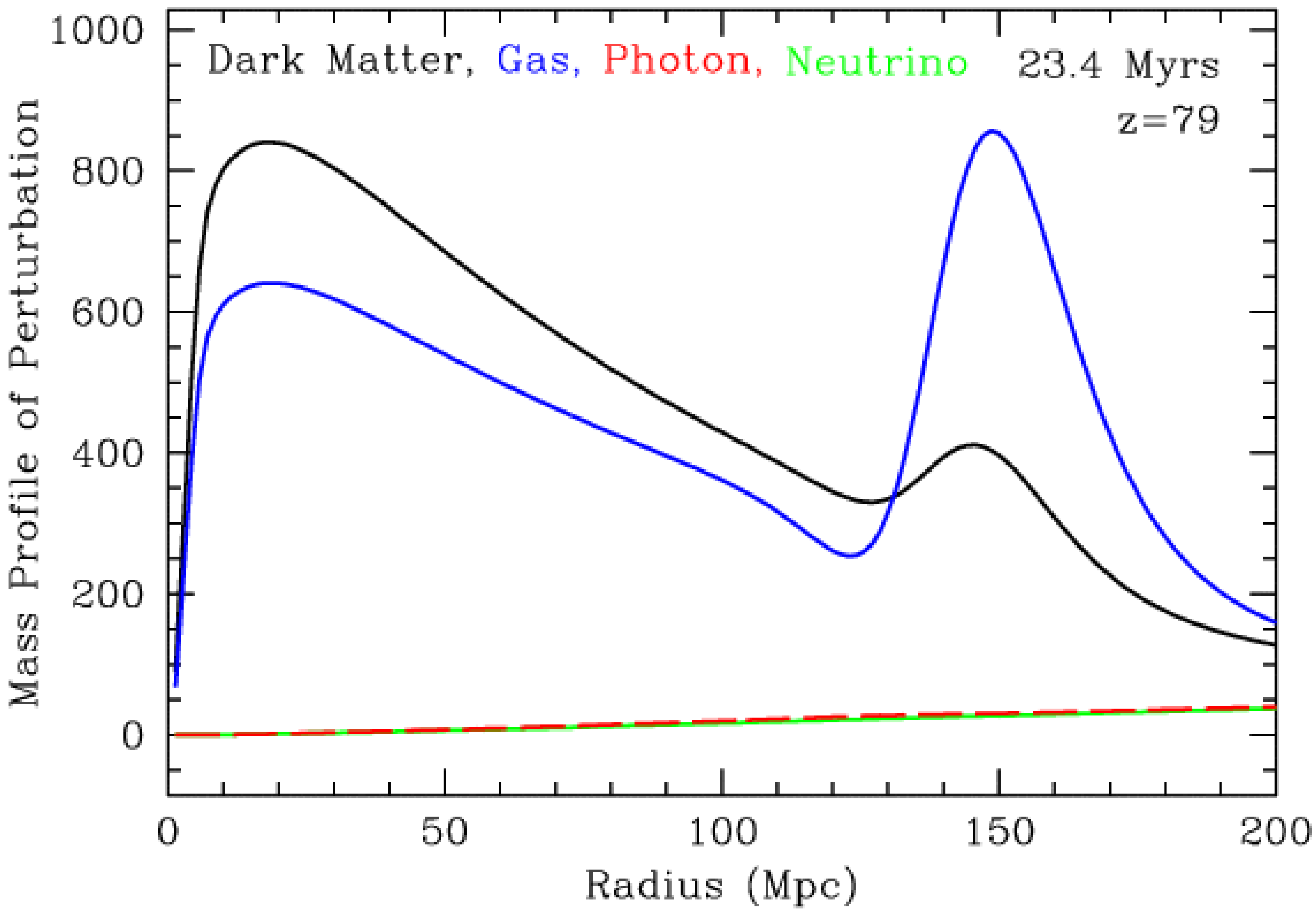

[credit: Daniel Eisenstein]

Baryonic Acoustic Oscillations

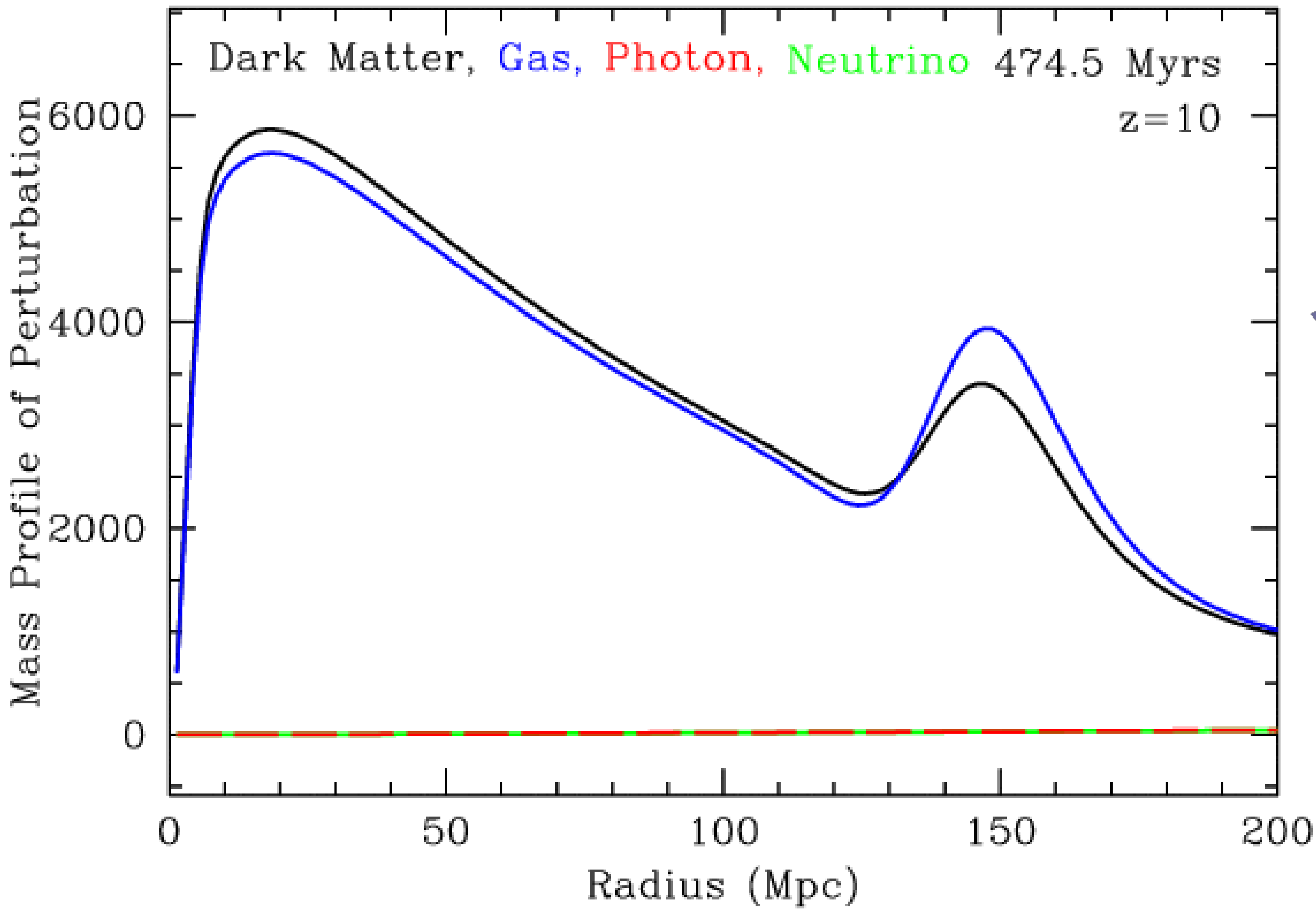

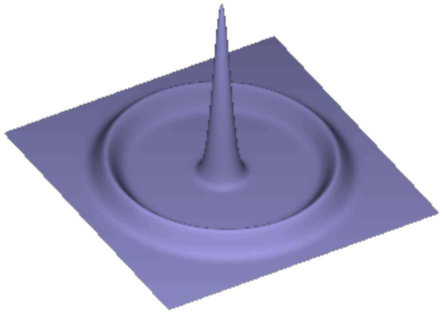

[credit: Daniel Eisenstein]

A standard ruler

we know the size of the "oscillation ring" very well from CMB observations

the galaxy 2-point function provides an "isotropic" measurement of the feature (if we get the cosmology right!)

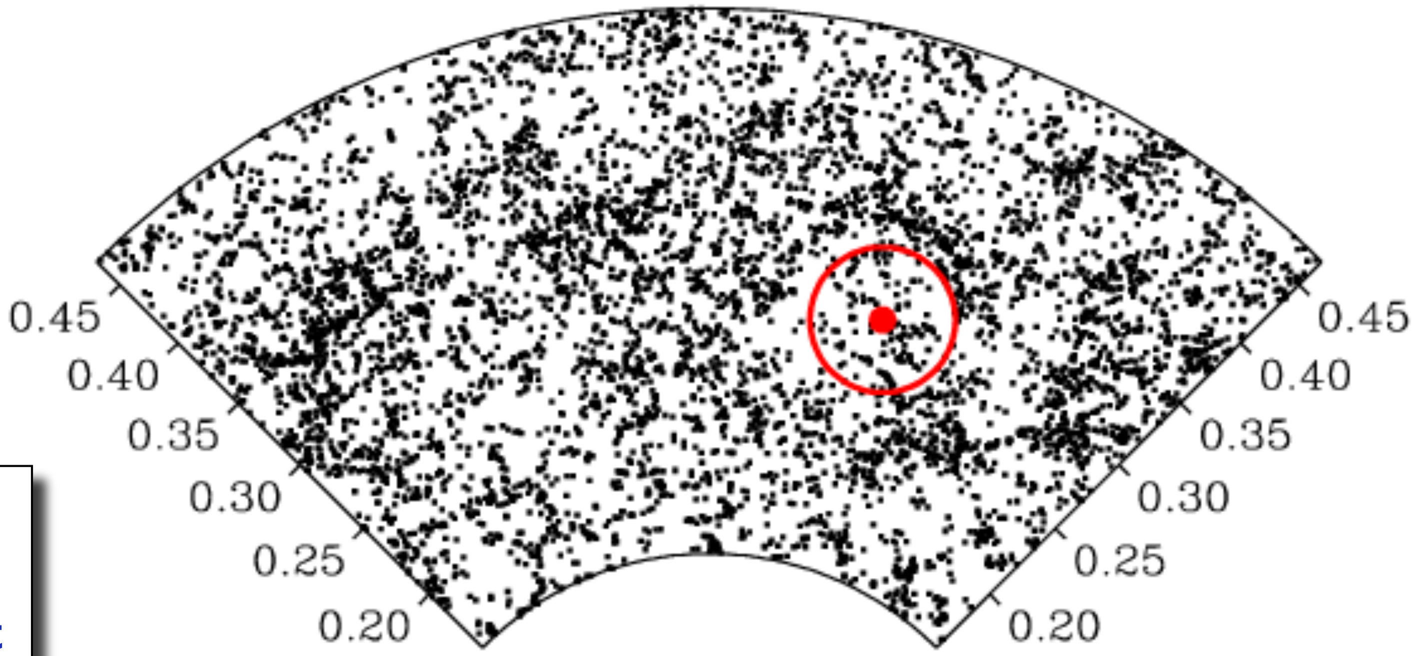

SDSS LRG sample:
first detection of the BAO peak
Eisenstein *et al.* (2005)

$$D_V(z) = \left[D_M(z)^2 \frac{cz}{H(z)} \right]^{1/3}$$

A standard ruler

we know the size of the "oscillation ring" very well from CMB observations

the galaxy 2-point function provides an "isotropic" measurement of the feature (if we get the cosmology right!)

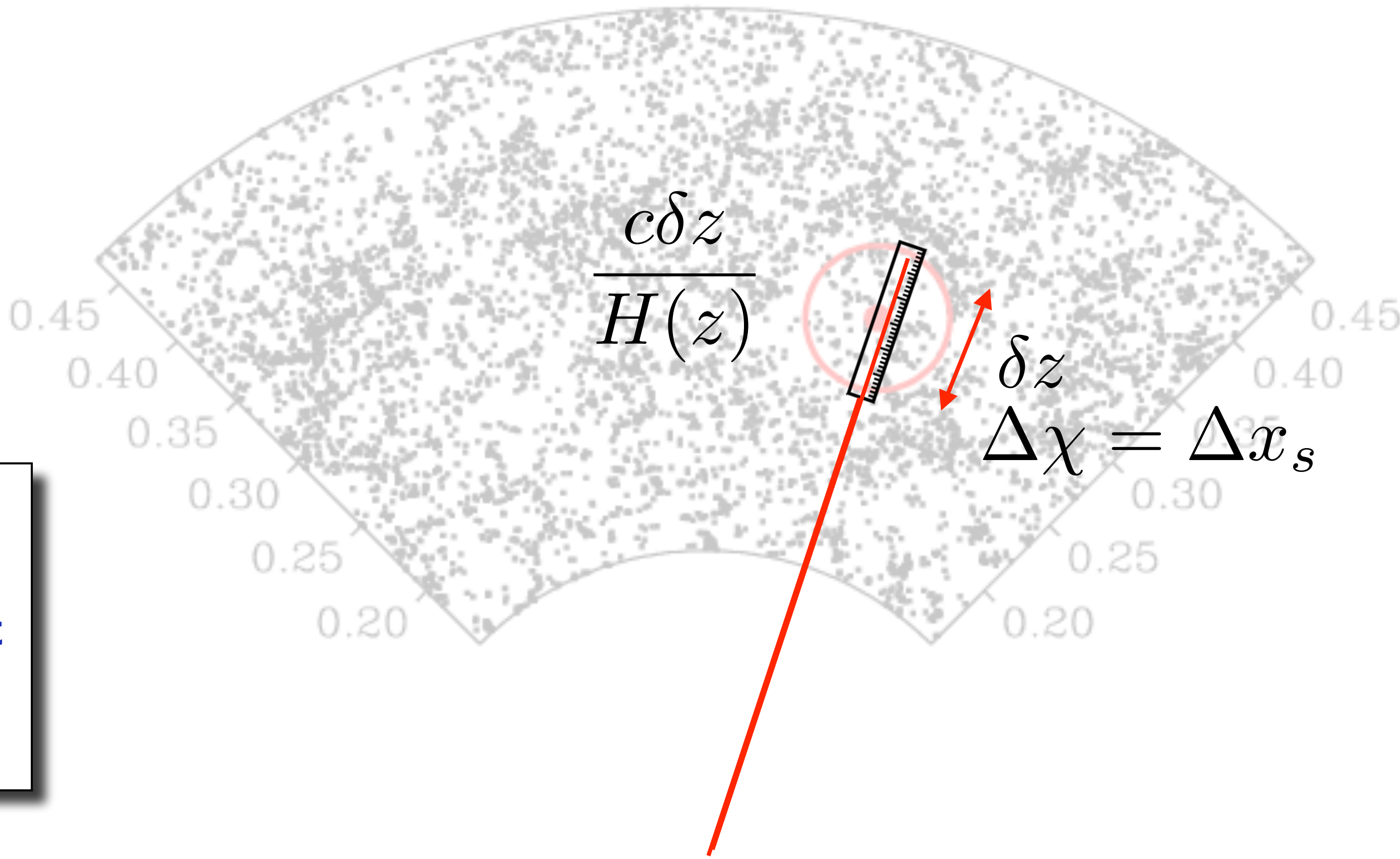

$$D_V(z) = \left[D_M(z)^2 \frac{cz}{H(z)} \right]^{1/3}$$

comoving distance along the line-of-sight

$$\chi = \int_{t_e}^{t_o} \frac{dt'}{a(t')} = \int_{a_e}^{a_o} \frac{da'}{H(a')} = \int_0^z \frac{dz'}{H(z')}$$

A standard ruler

we know the size of the "oscillation ring" very well from CMB observations

the galaxy 2-point function provides an "isotropic" measurement of the feature (if we get the cosmology right!)

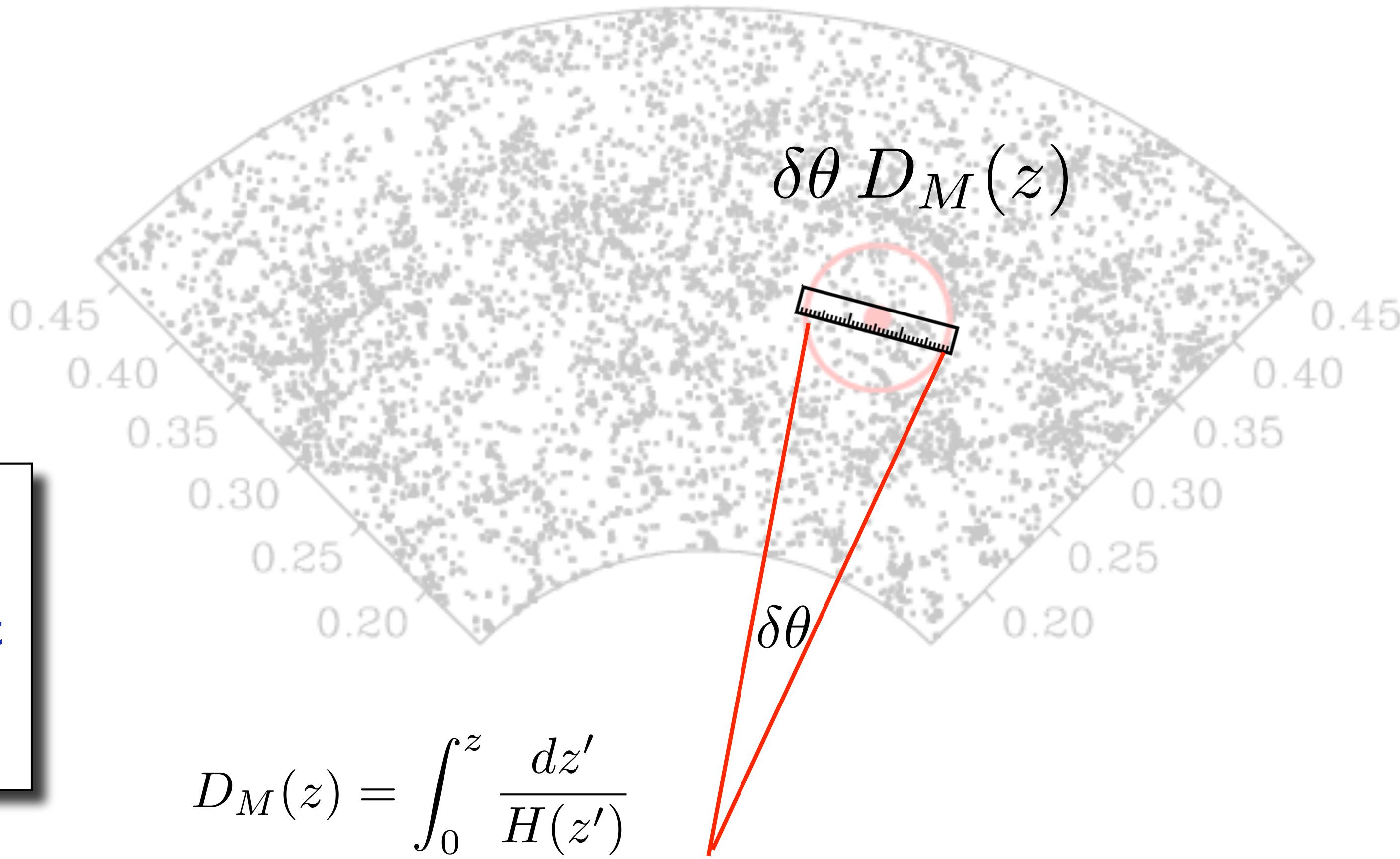

$$D_M(z) = \int_0^z \frac{dz'}{H(z')}$$

comoving angular diameter distance

$$D_V(z) = \left[D_M(z)^2 \frac{cz}{H(z)} \right]^{1/3}$$

BAO: how well do we measure them?

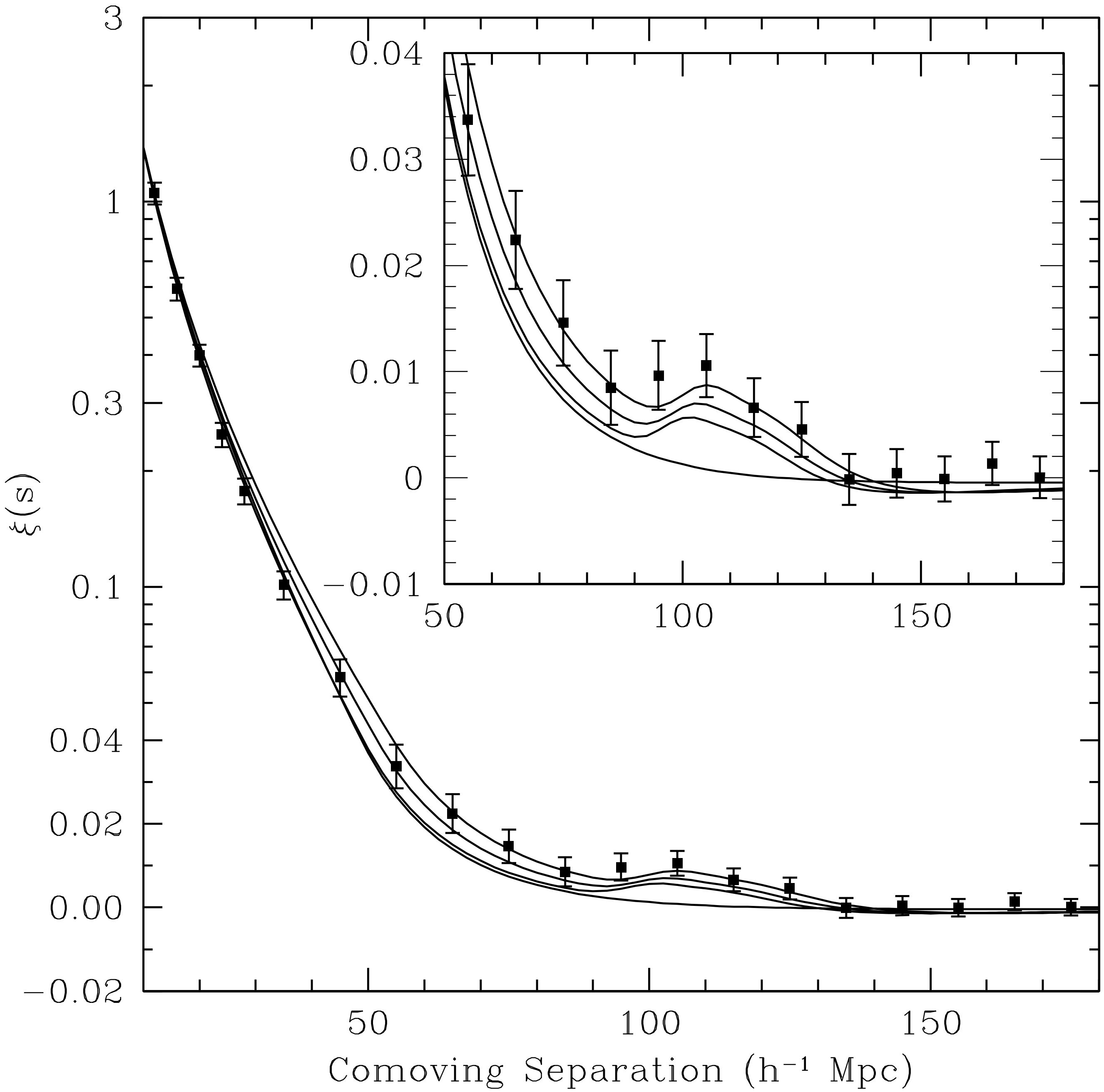

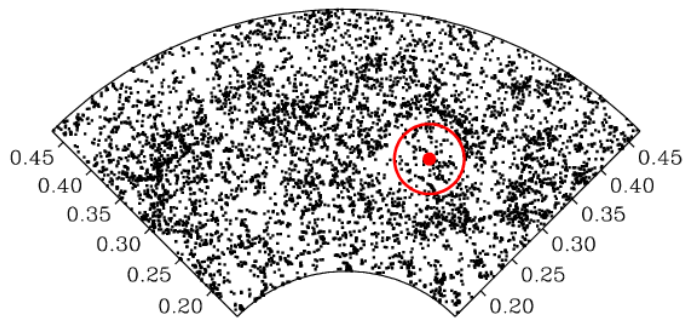

SDSS LRG sample:
first detection of the BAO peak
Eisenstein *et al.* (2005)

BAO: how well do we measure them?

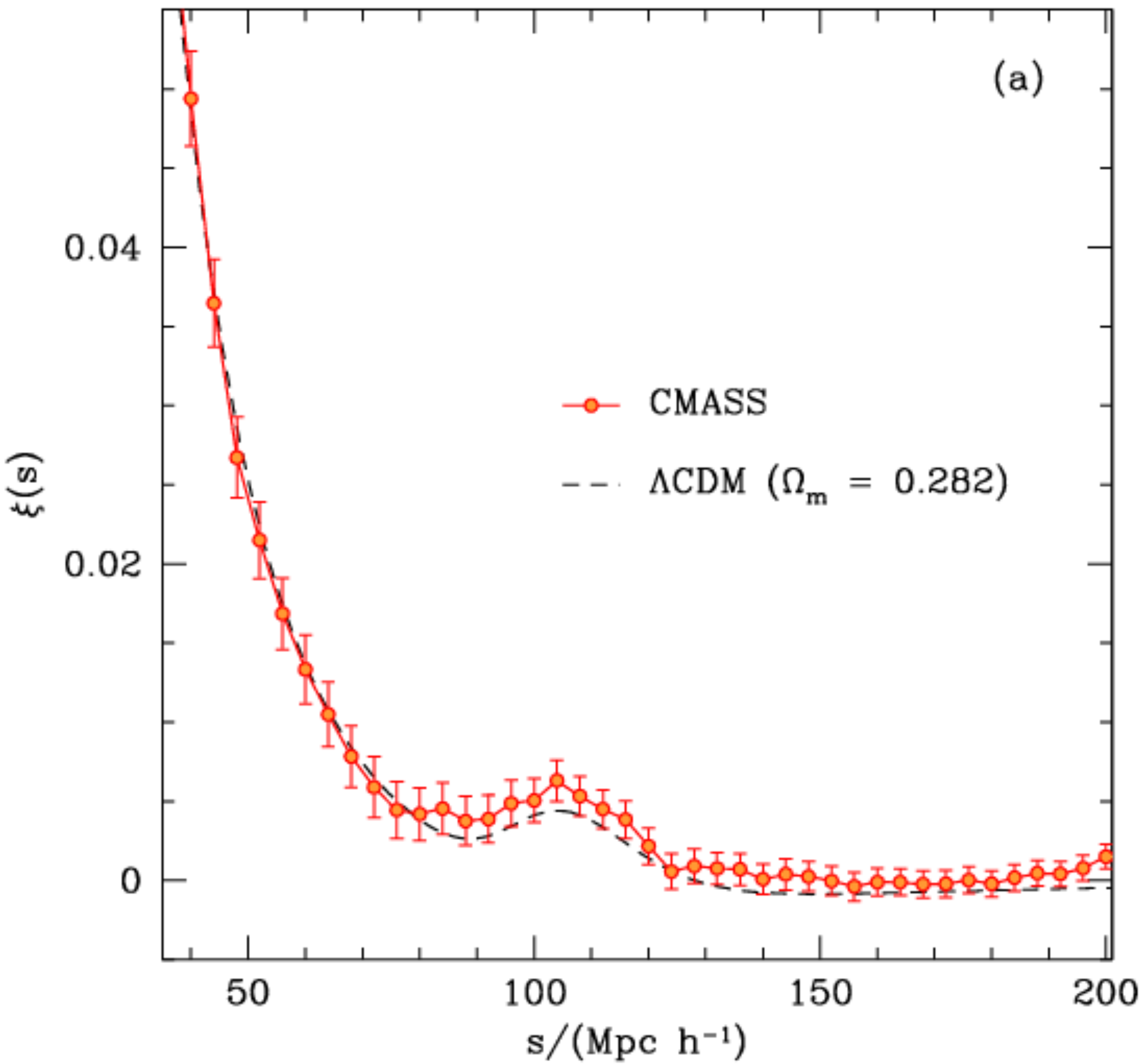

Baryon Oscillation Spectroscopic Survey
BOSS

1.5 million galaxies
up to z = 0.7

Anderson *et al.* (2012)

BAO: how well do we measure them?

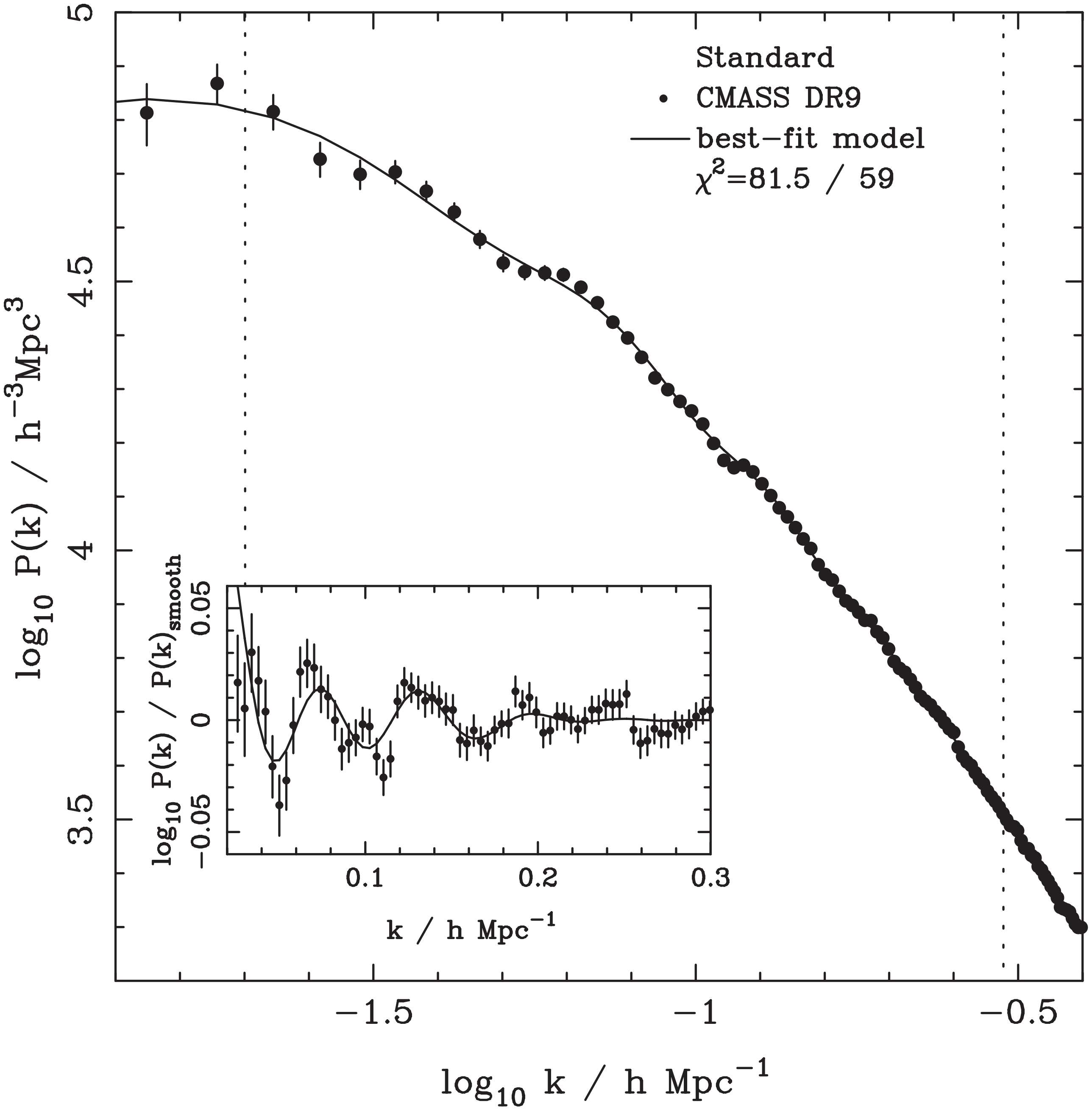

Baryon Oscillation Spectroscopic Survey
BOSS

1.5 million galaxies
up to z = 0.7

Anderson *et al.* (2012)

Constraints from BAO

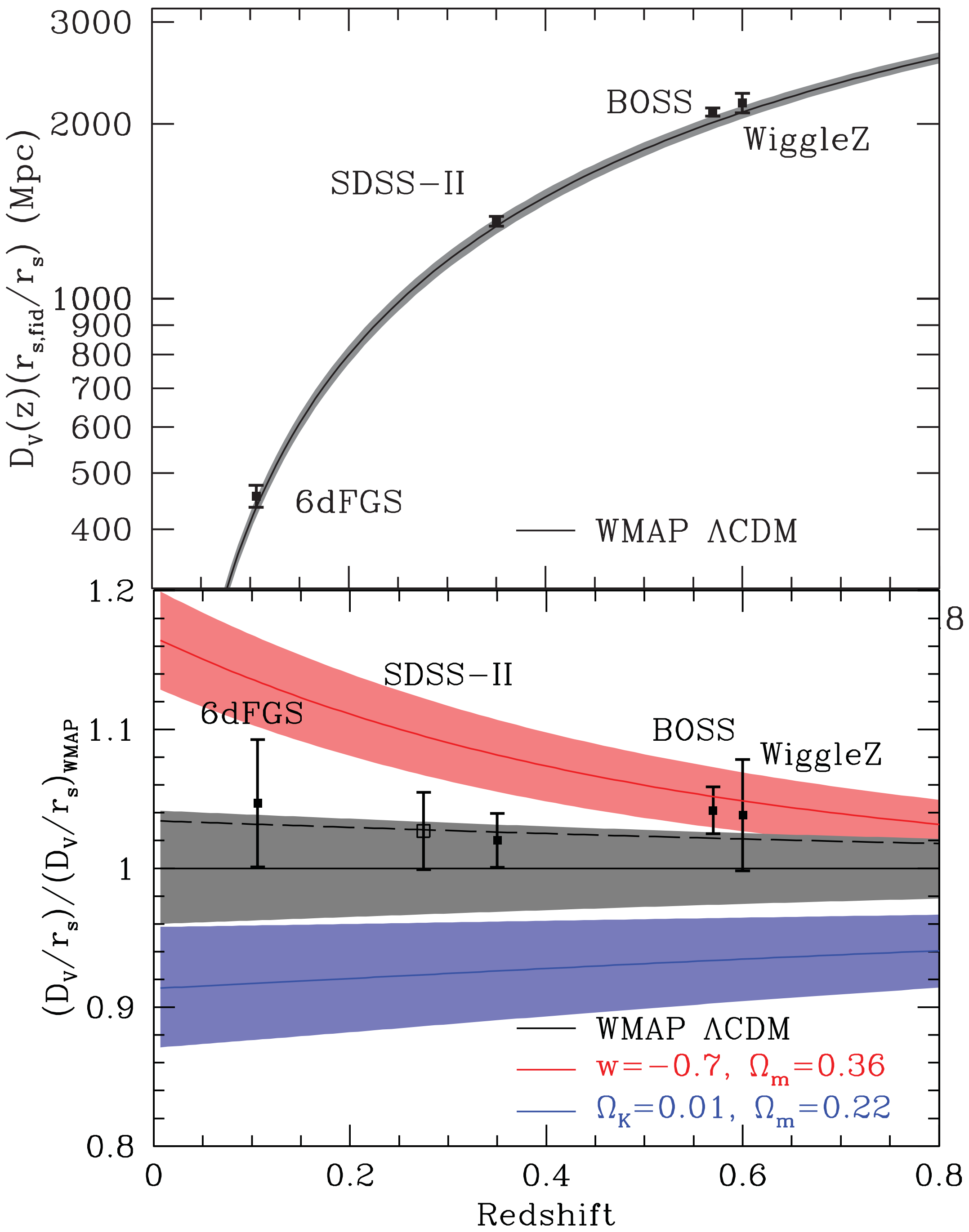

$$D_V(z) = \left[D_M(z)^2 \frac{cz}{H(z)} \right]^{1/3}$$

$$D_M(z) = \int_0^z \frac{dz'}{H(z')}$$

Anderson *et al.* (2012)
BOSS collaboration

Constraints from BAO

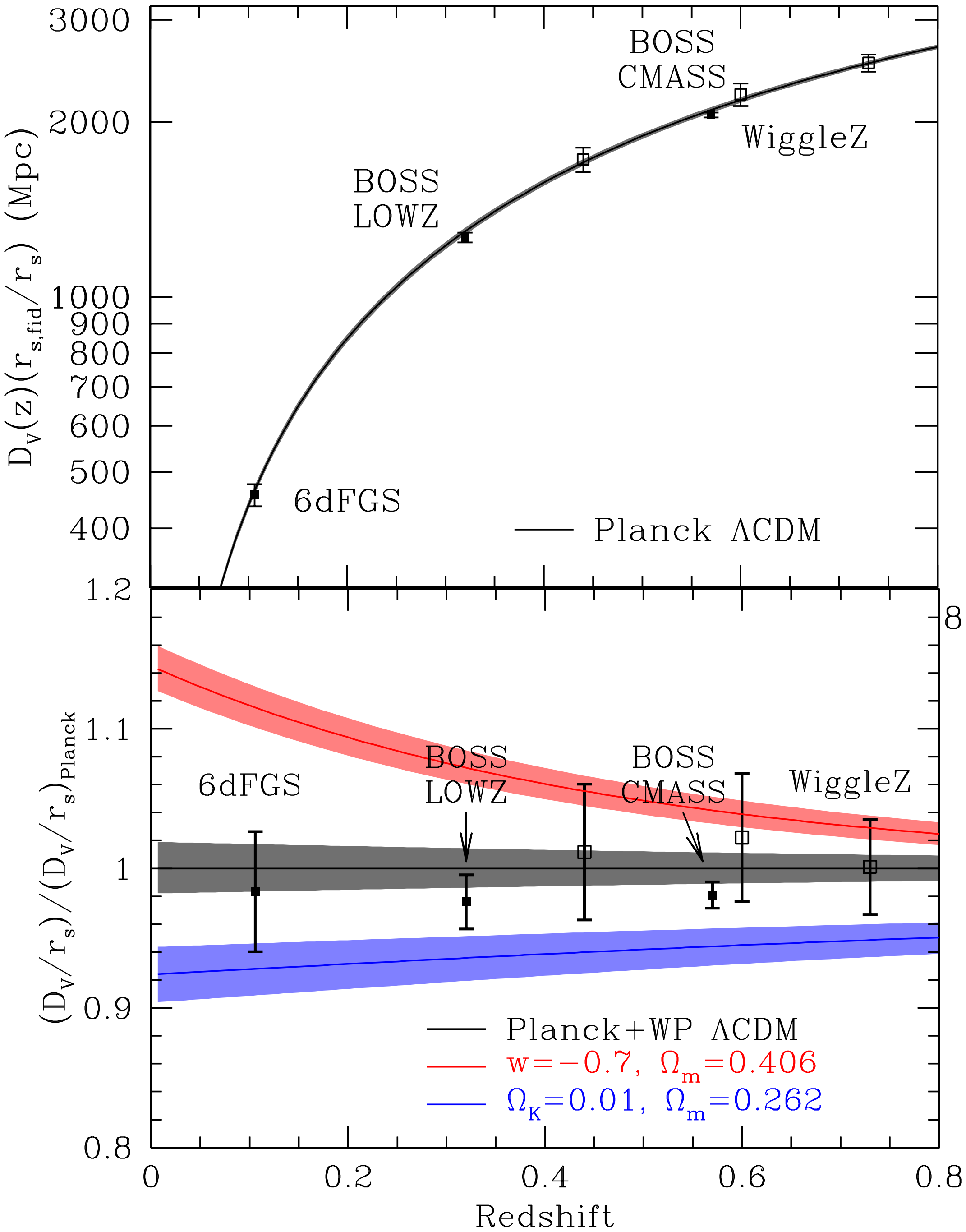

$$D_V(z) = \left[D_M(z)^2 \frac{cz}{H(z)} \right]^{1/3}$$

$$D_M(z) = \int_0^z \frac{dz'}{H(z')}$$

Anderson *et al.* (2014)
BOSS collaboration

Constraints from BAO

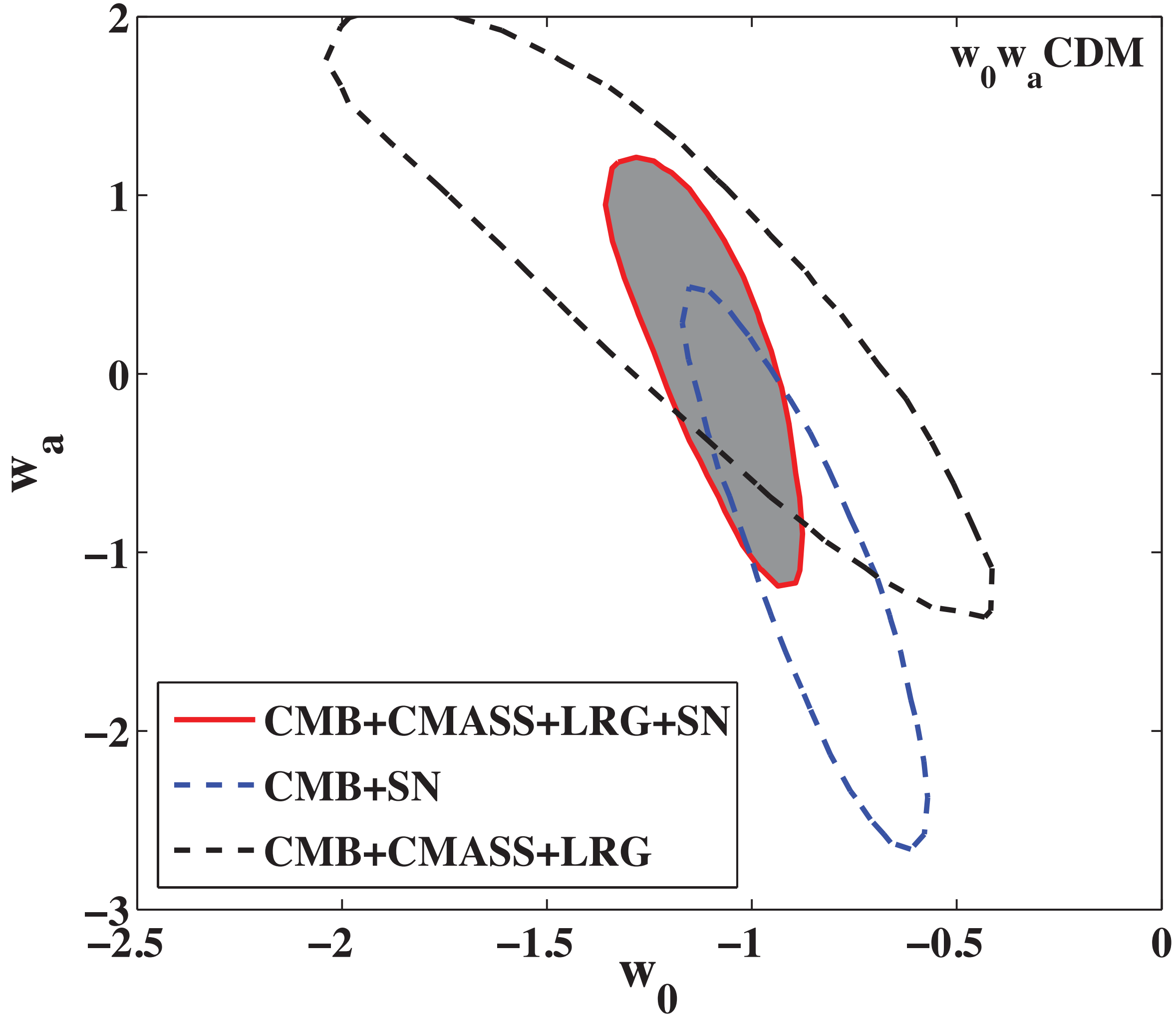

Constraints on a *time-dependent* **Dark Energy equation of state:**

$$w(a) = w_0 + (1 - a)\, w_a$$

Anderson *et al.* (2012)
BOSS collaboration

Constraints from BAO

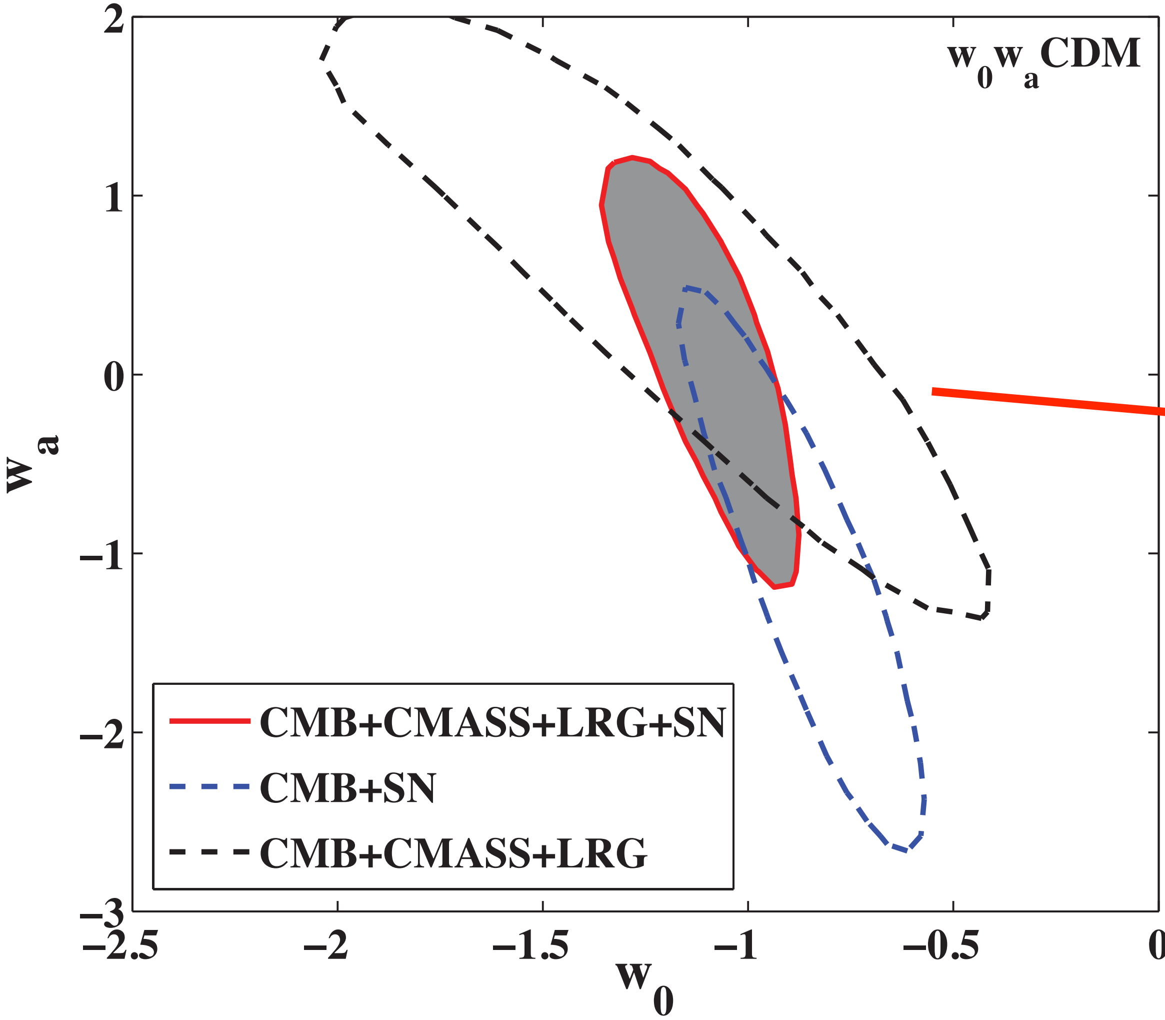

Constraints on a *time-dependent* **Dark Energy equation of state:**

$$w(a) = w_0 + (1 - a)\, w_a$$

This area is the Figure of Merit adopted by the Dark Energy Task Force!

Anderson *et al.* (2012)
BOSS collaboration

Constraints from BAO

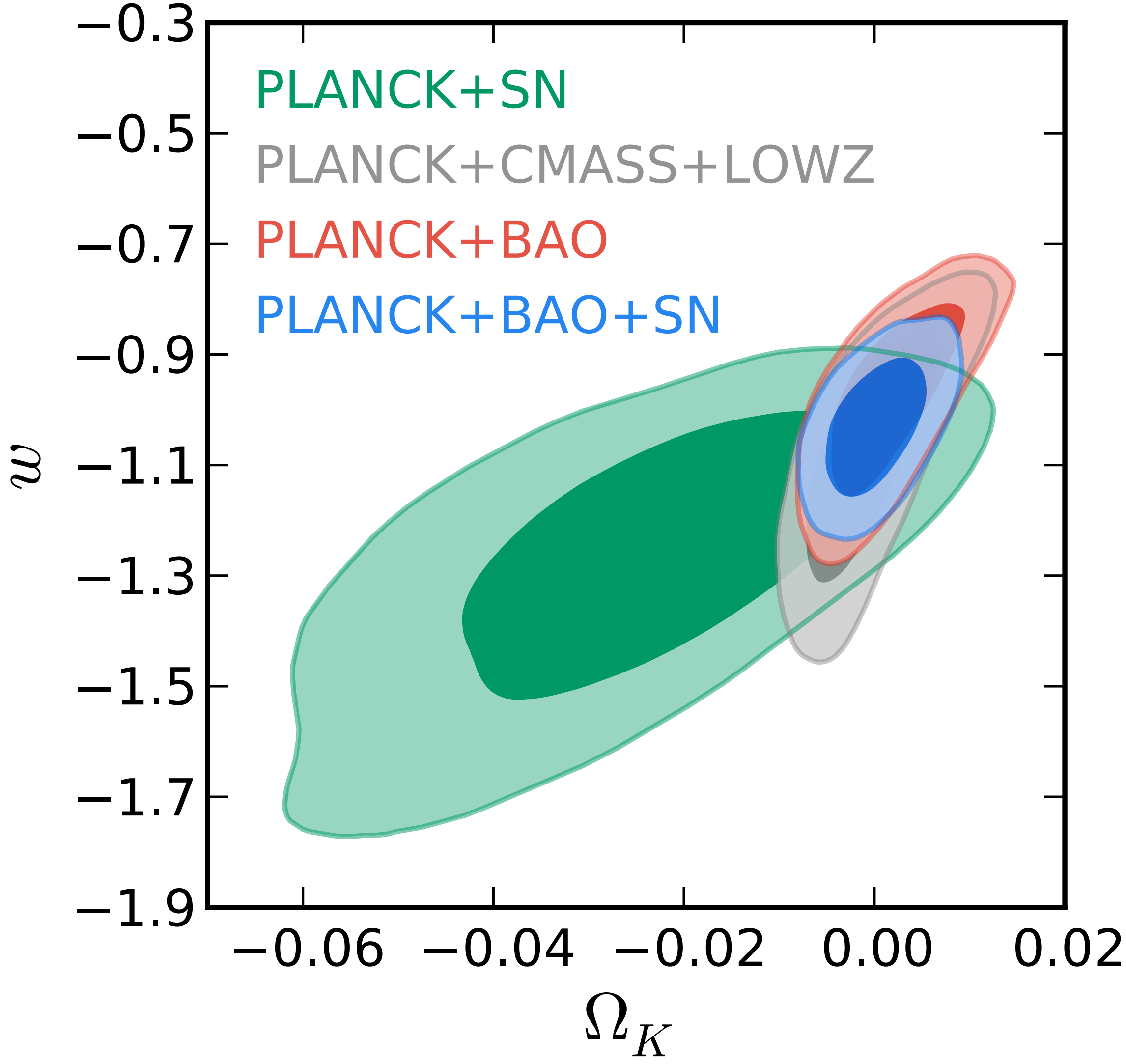

Simultaneous constraints on a the **Dark Energy equation of state** and **curvature**

Anderson *et al.* (2014)
BOSS collaboration

The future

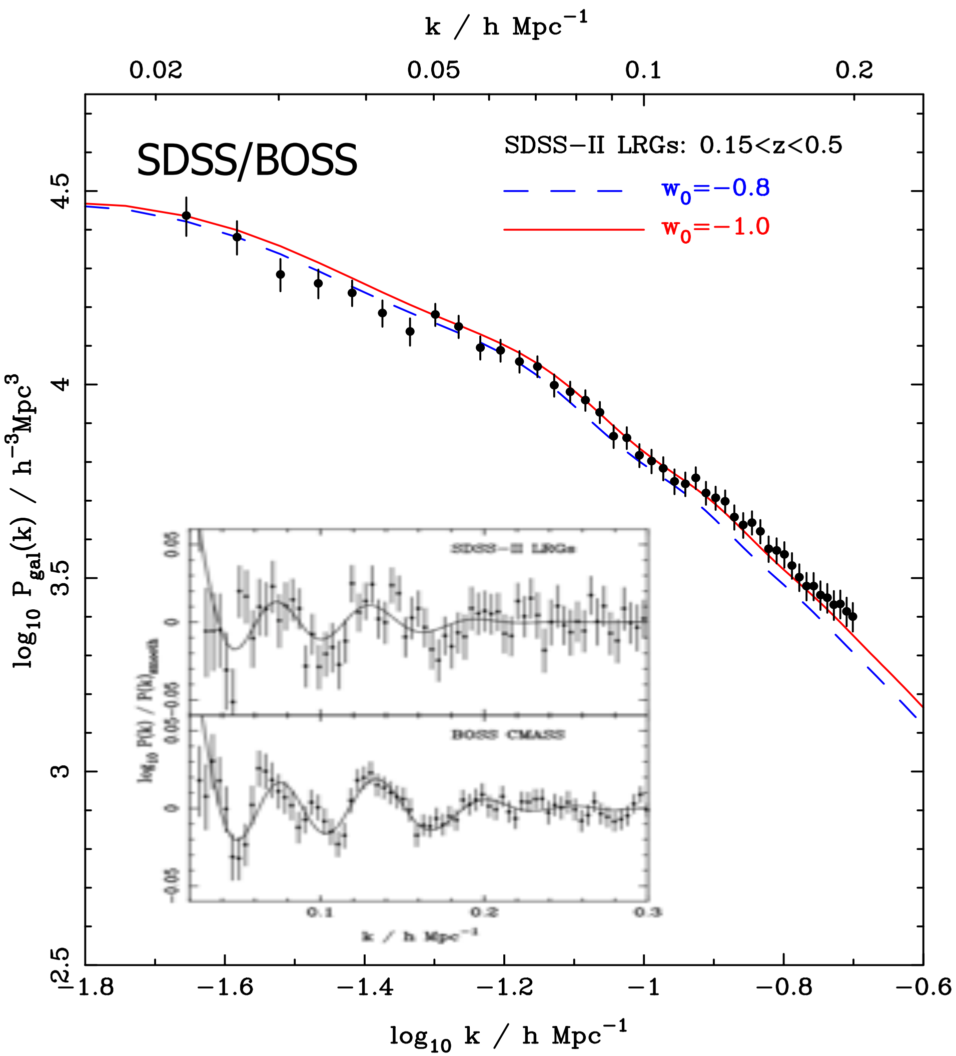

SDSS LRGs at z~0.35

Total effective volume
V_{eff} = 0.26 Gpc^{3}h^{-3}

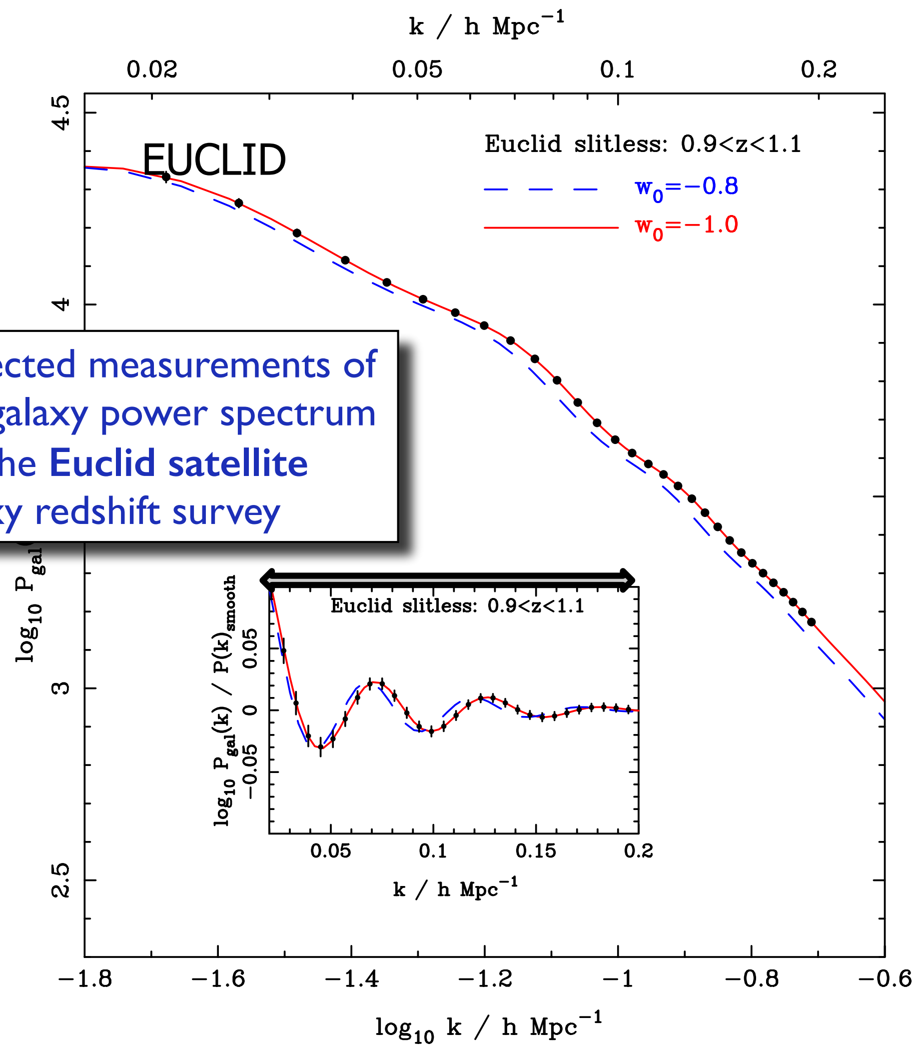

Expected measurements of the galaxy power spectrum for the **Euclid satellite** galaxy redshift survey

20% of the Euclid slitless data at z~1

Total effective volume (of Euclid)
V_{eff} = 19.7 Gpc^{3}h^{-3}

[courtesy of G. Guzzo]

The future

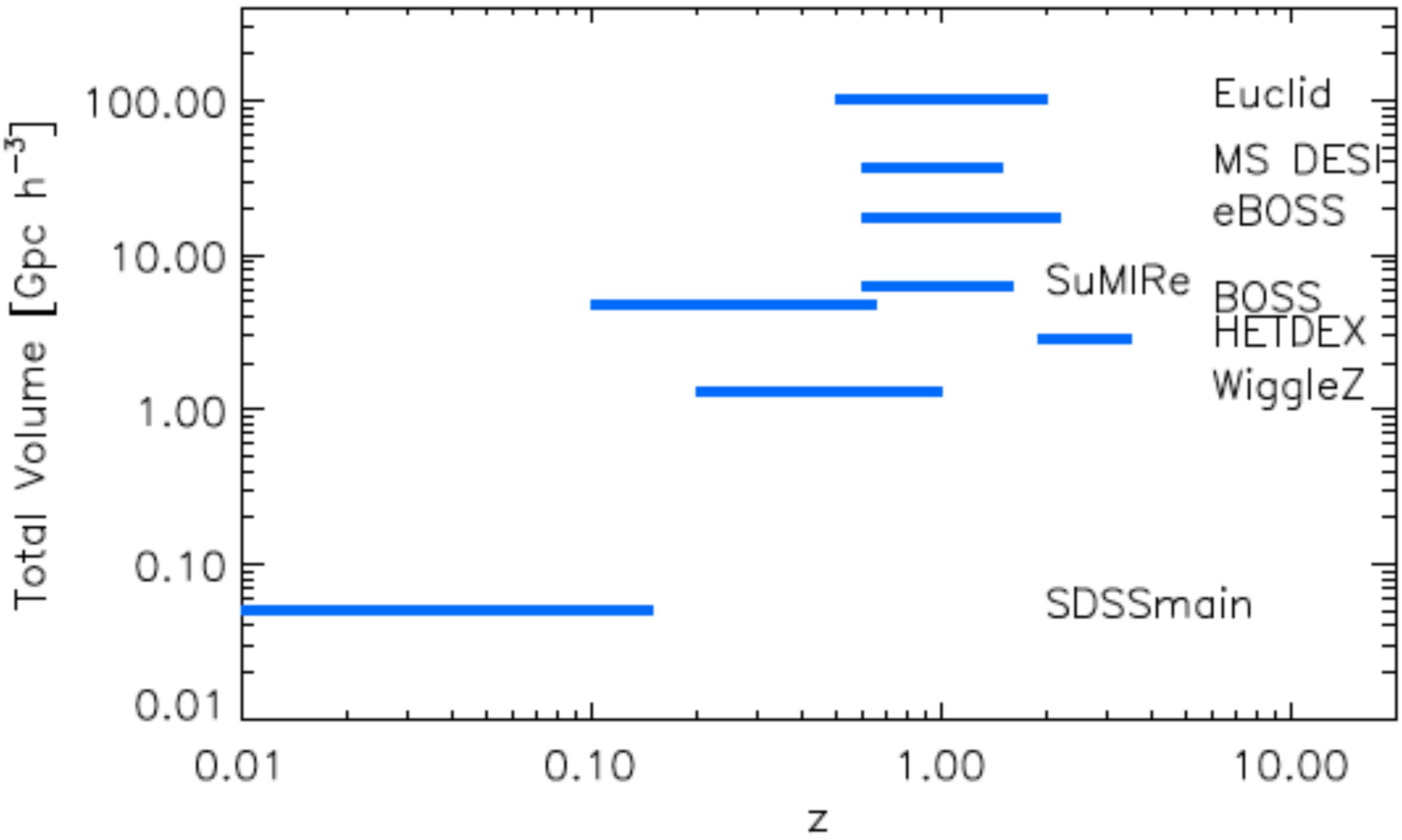

[Euclid Theory Group]

The future

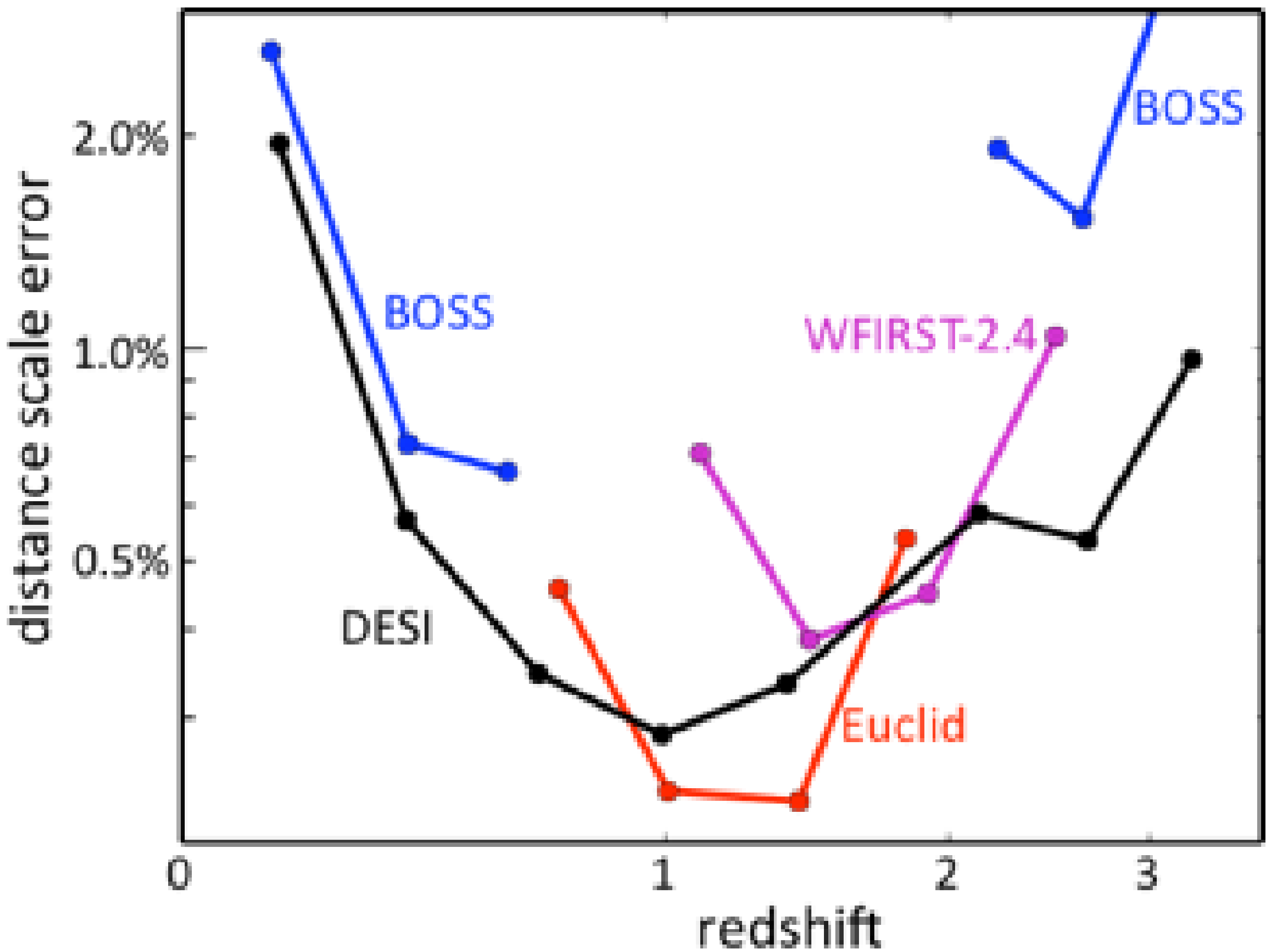

[D. Eisenstein]

The future

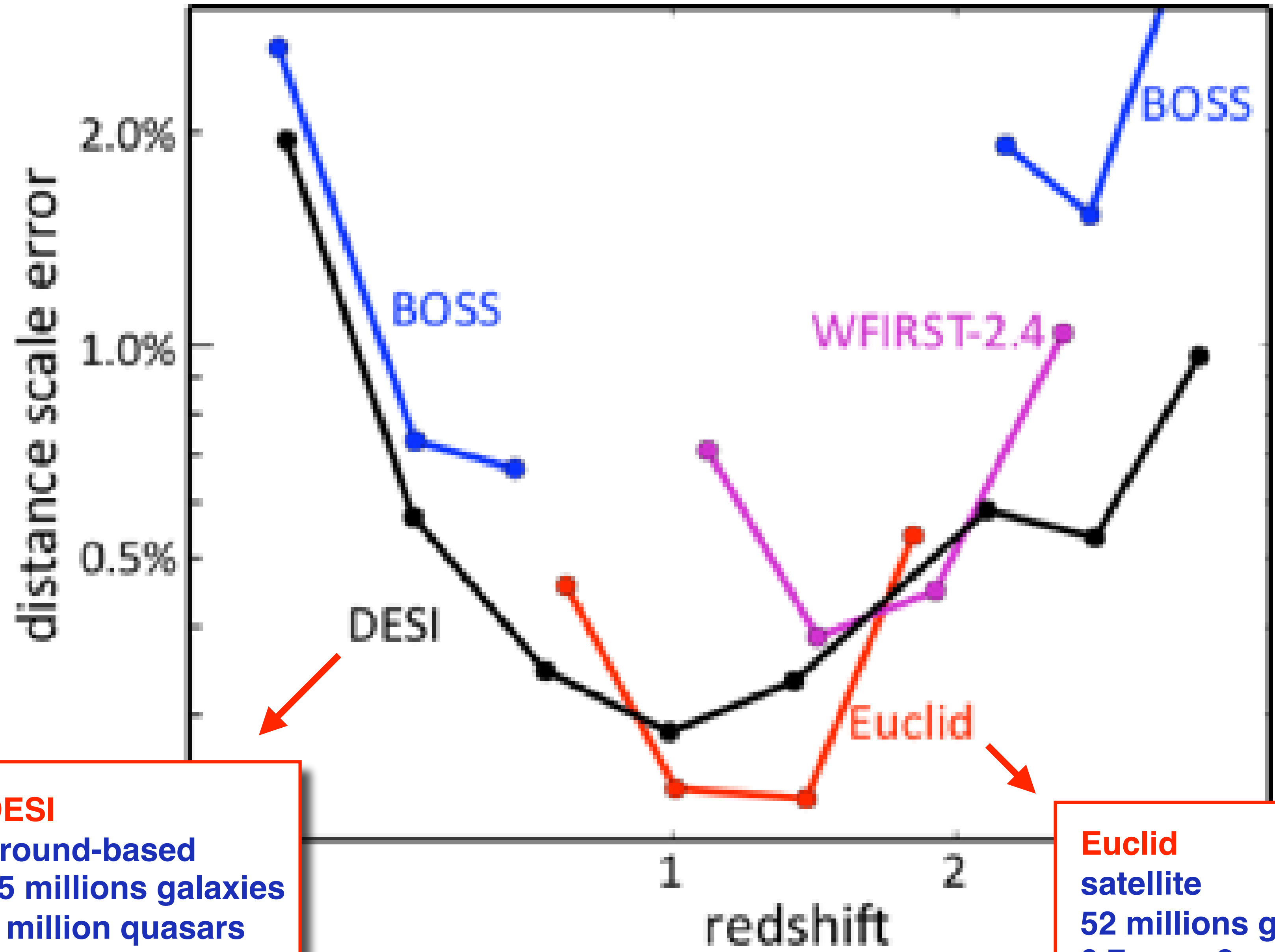

DESI
ground-based
25 millions galaxies
2 million quasars
z < 3.5

Euclid
satellite
52 millions galaxies
0.7 < z < 2

[D. Eisenstein]

Redshift-space distortions

Redshift-space

Galaxies are observed in **redshift space** *not* in real space

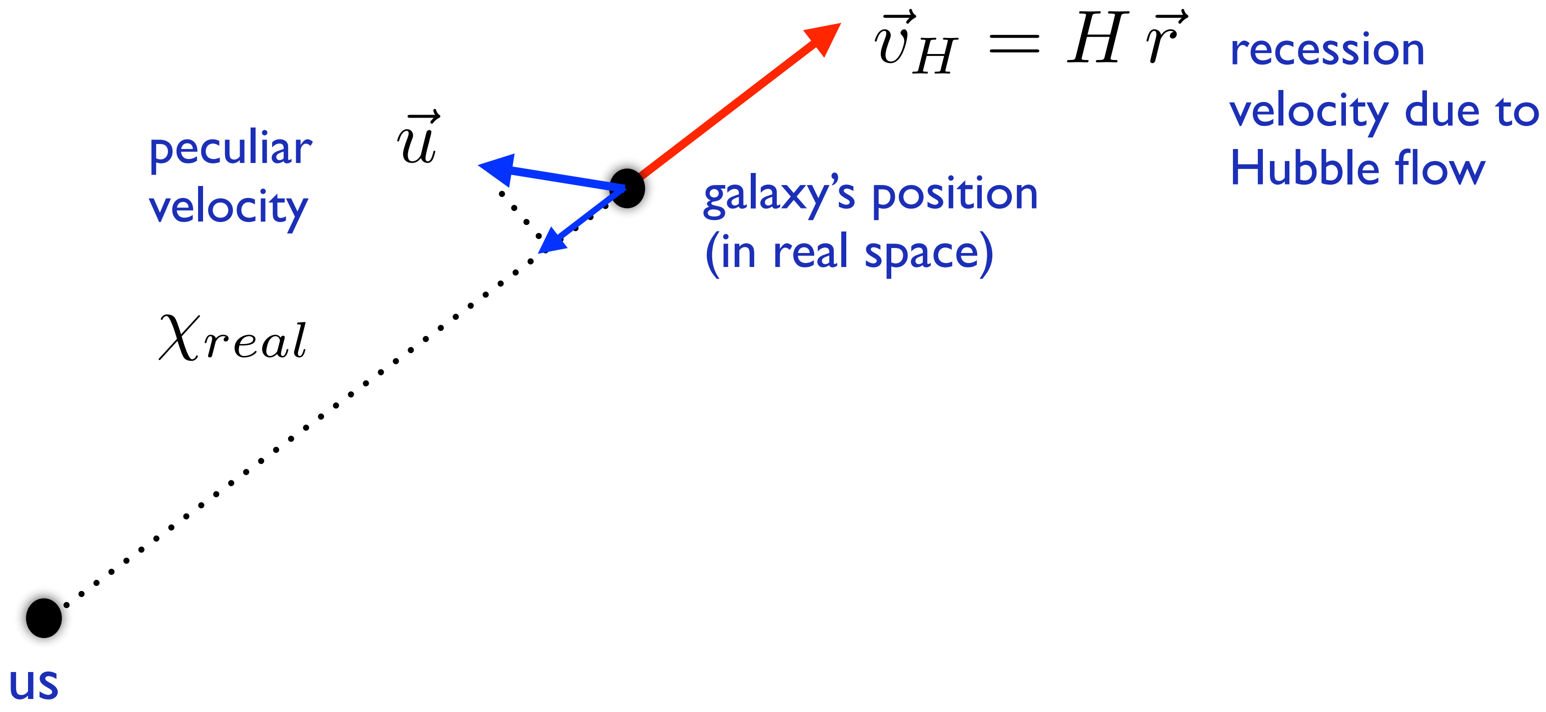

Redshift-space

Galaxies are observed in **redshift space** *not* in real space

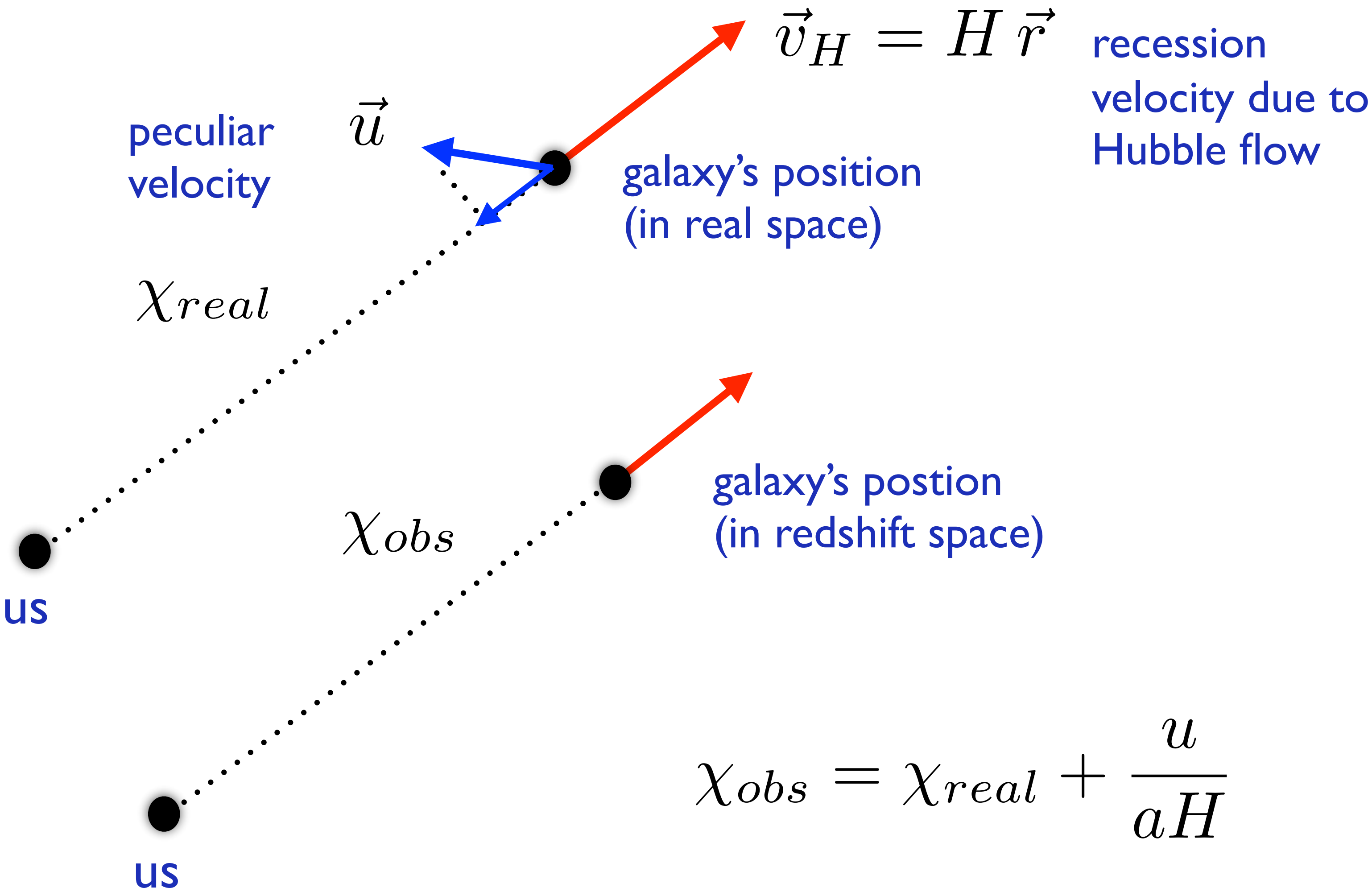

$$\chi_{obs} = \chi_{real} + \frac{u}{aH}$$

Redshift-Space Distortions (RSD)

Two effects:

1. **Kaiser effect** on large scales
2. **Finger-of-God effect** on small scales

Kaiser effect

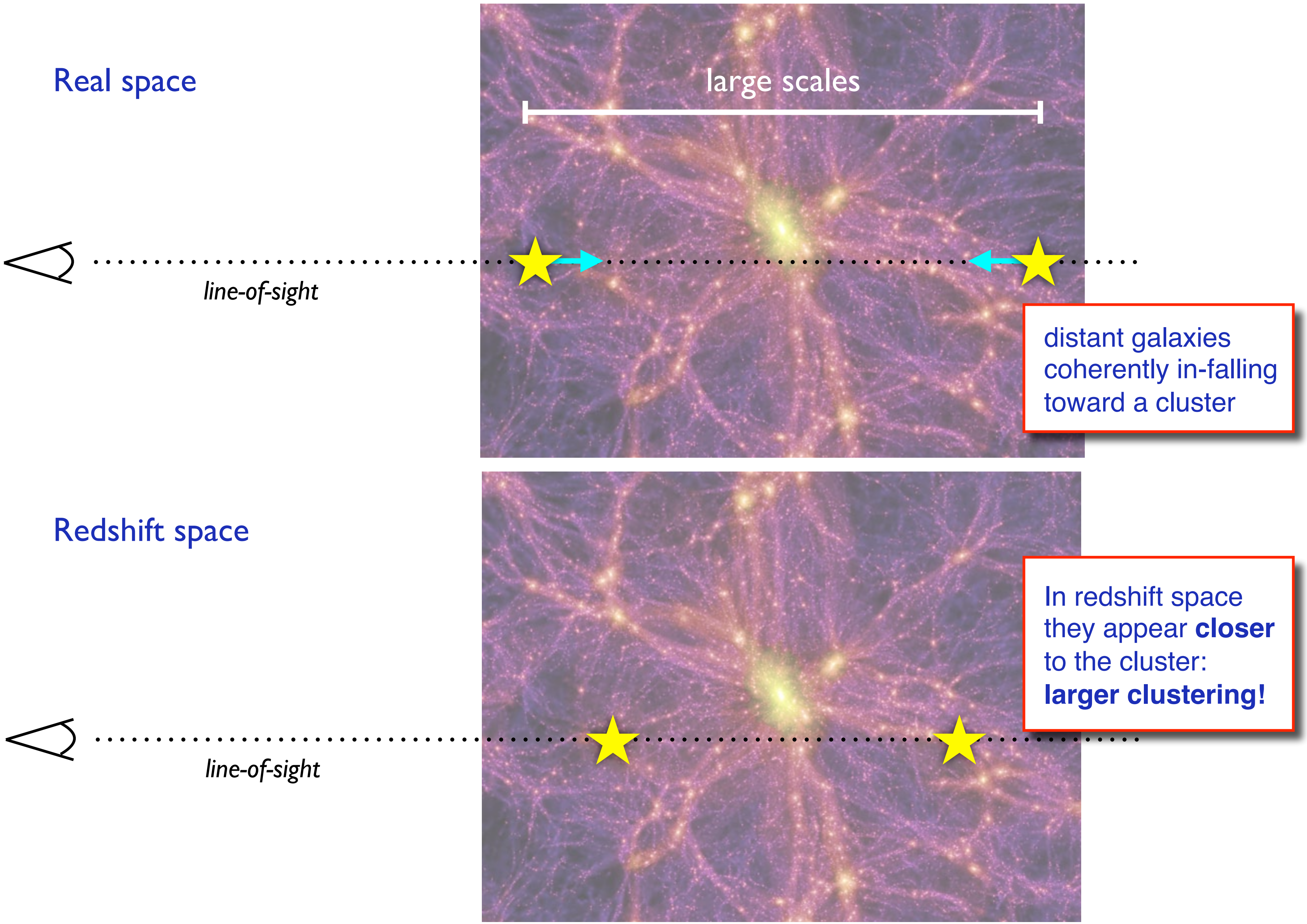

Kaiser effect

Redshift-space galaxy **overdensity**

$$\delta^s_{g,\vec{k}} = \delta_{g,\vec{k}} + \mu_k^2 \theta_{\vec{k}} \simeq \left(1 + \frac{f}{b}\,\mu_k^2\right) b\,\delta_{\vec{k}}$$

correction due to line-of-sight component of peculiar velocity

$$\frac{\partial \delta}{\partial \tau} + \theta = 0$$ continuity eq.

$$\boxed{P_s(\vec{k}) = \left(1 + \frac{f}{b}\,\mu_k^2\right)^2 P_g(k)}$$

the **redshift-space power spectrum** is **anisotropic**!
(and so is the correlation function)

$$f \equiv \frac{d \ln D(a)}{d \ln a} = \Omega_m^\gamma(z)$$

enhanced clustering along the line-of-sight, proportional to the **growth rate**

Finger-of-God effect

Real space

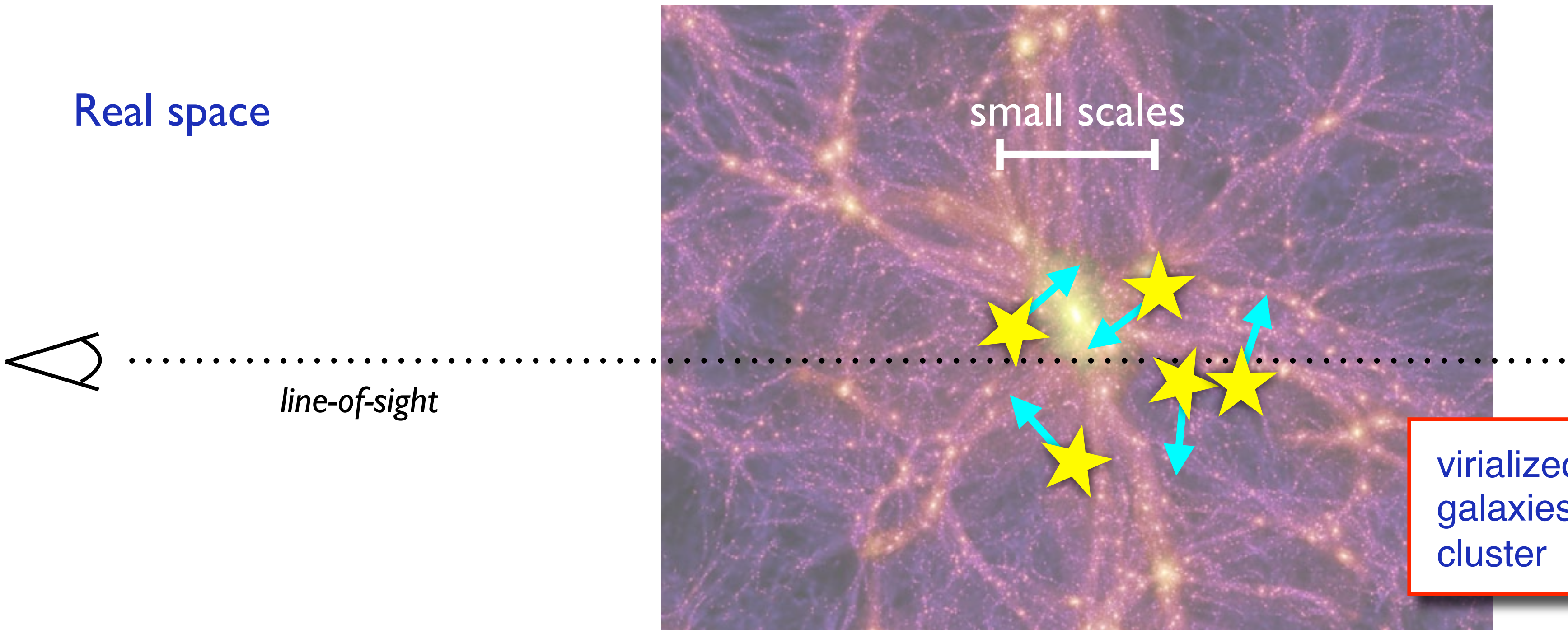

virialized motion of galaxies *within* a cluster

Redshift space

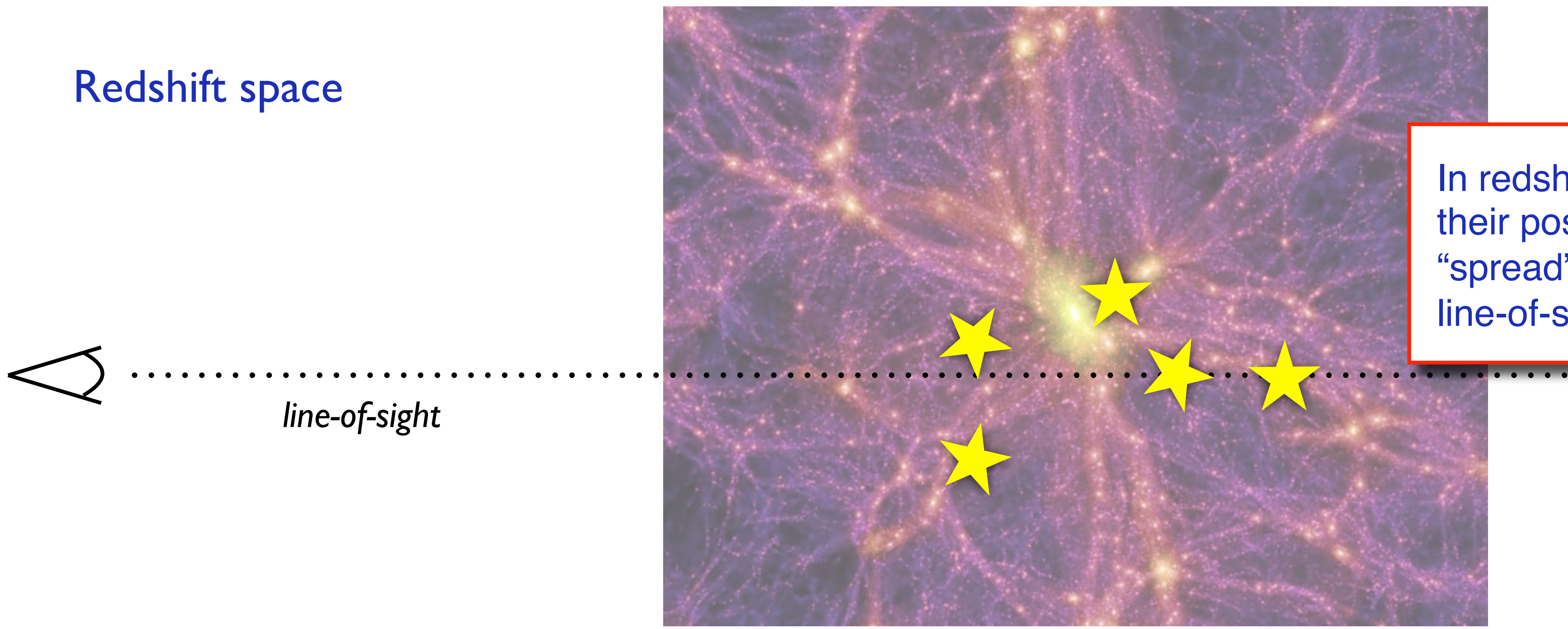

In redshift space their positions are “spread” along the line-of-sight

Finger-of-God effect

Redshift space

Real space

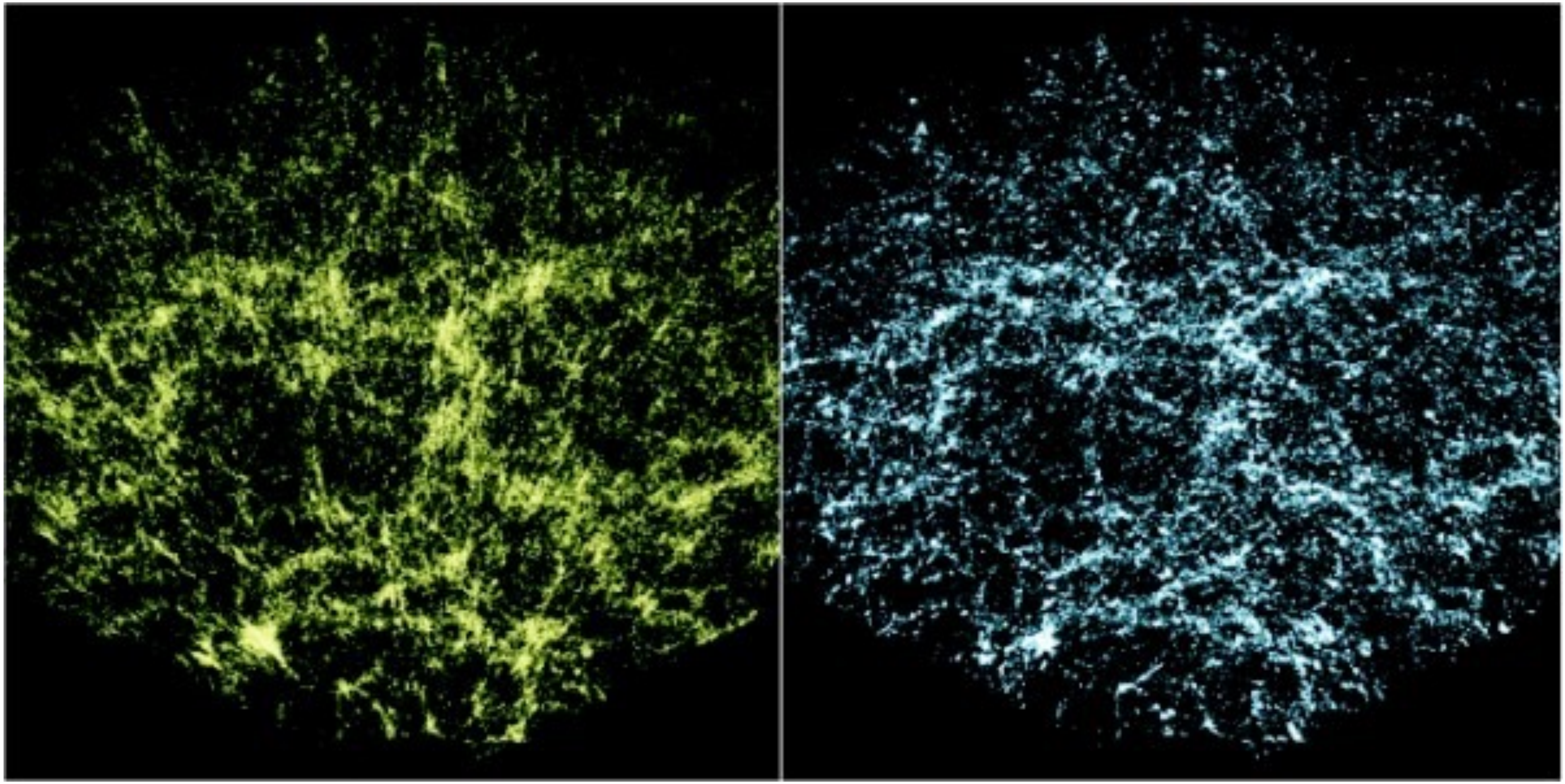

[SubbaRao *et al.* (2008)]

The galaxy power spectrum in redshift space

$$P_s(\vec{k}) = P_g(k)\left(1 + \frac{f}{b}\mu_k^2\right)^2 e^{-k^2\mu_k^2\sigma^2}$$

Kaiser effect   Finger-of-God effect

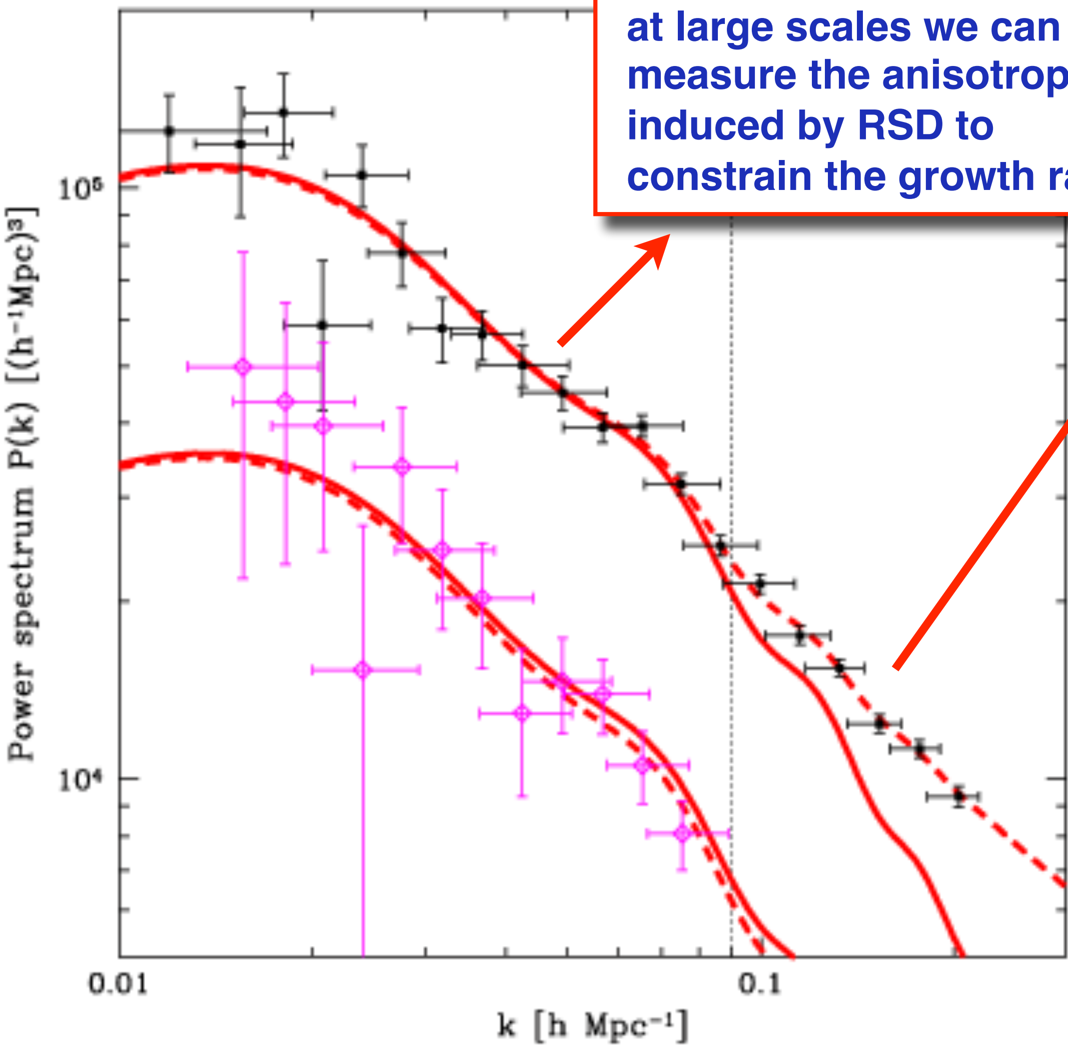

at large scales we can measure the anisotropy induced by RSD to constrain the growth rate

at small scales, non-linear bias is degenerate with non-linear corrections to the matter power spectrum **and with redshift-space distortions**

The galaxy correlation function in redshift space

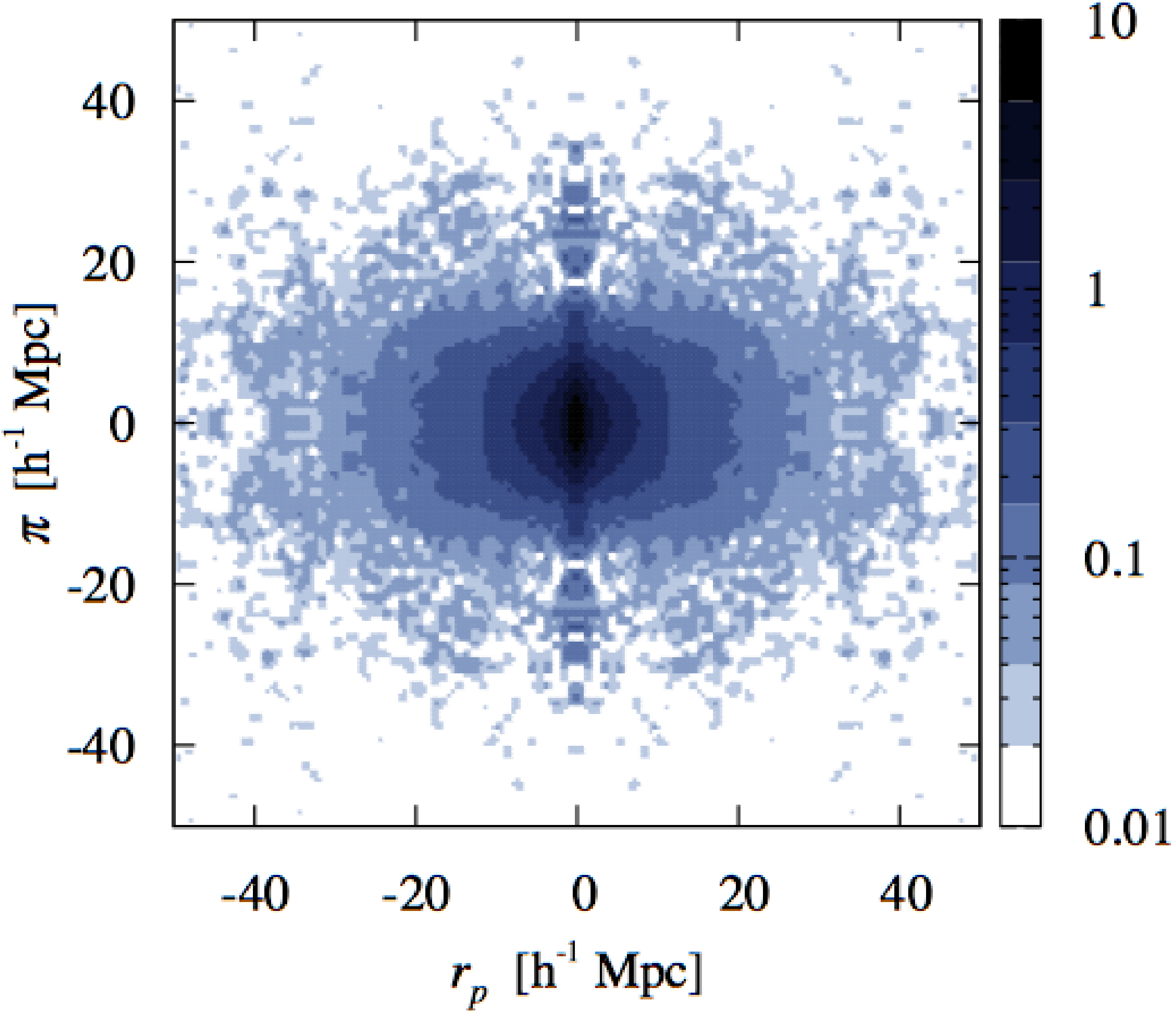

$\xi(r_p, \pi)$

De La Torre *et al.* (2013)
VIPERS collaboration

Constraining the growth rate

S. de la Torre et al.: Galaxy clustering and redshift-space distortions in VIPERS

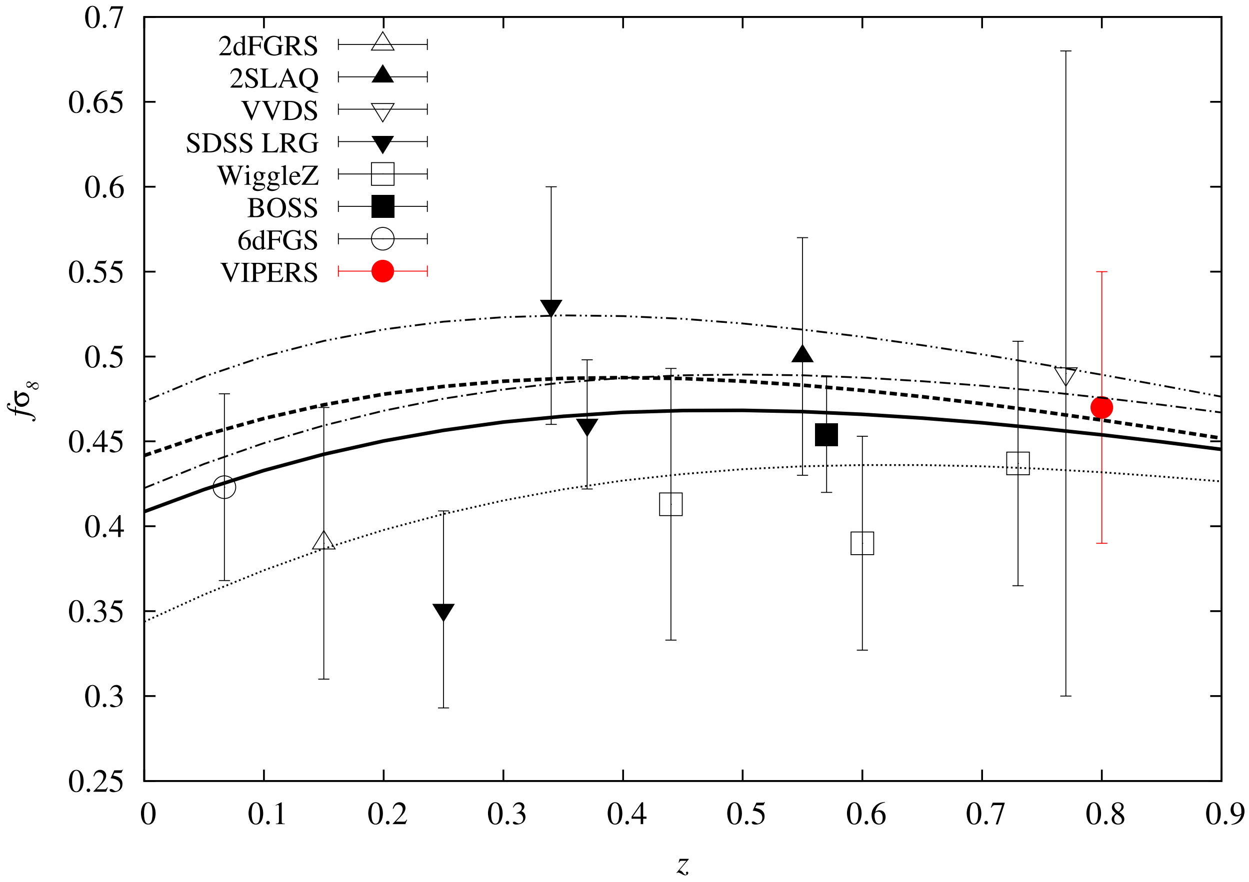

Fig. 19. A plot of $f\sigma_8$ versus redshift, showing VIPERS result contrasted with a compilation of recent measurements. The previous results from 2dFGRS (Hawkins et al. 2003), 2SLAQ (Ross et al. 2007), VVDS (Guzzo et al. 2008), SDSS LRG (Cabré & Gaztañaga 2009; Samushia et al. 2012), WiggleZ (Blake et al. 2012), BOSS (Reid et al. 2012), and 6dFGS (Beutler et al. 2012) surveys are shown with the different symbols (see inset). The thick solid (dashed) curve corresponds to the prediction for General Relativity in a ΛCDM model with WMAP9 (*Planck*) parameters, while the dotted, dot-dashed, and dot-dot-dashed curves are respectively Dvali-Gabadaze-Porrati (Dvali et al. 2000), coupled dark energy, and $f(R)$ model expectations. For these models, the analytical growth rate predictions given in di Porto et al. (2012) have been used.

$$f \equiv \frac{d \ln D(a)}{d \ln a} = \Omega_m^\gamma(z)$$

De La Torre *et al.* (2013)
VIPERS collaboration

Constraining gravity

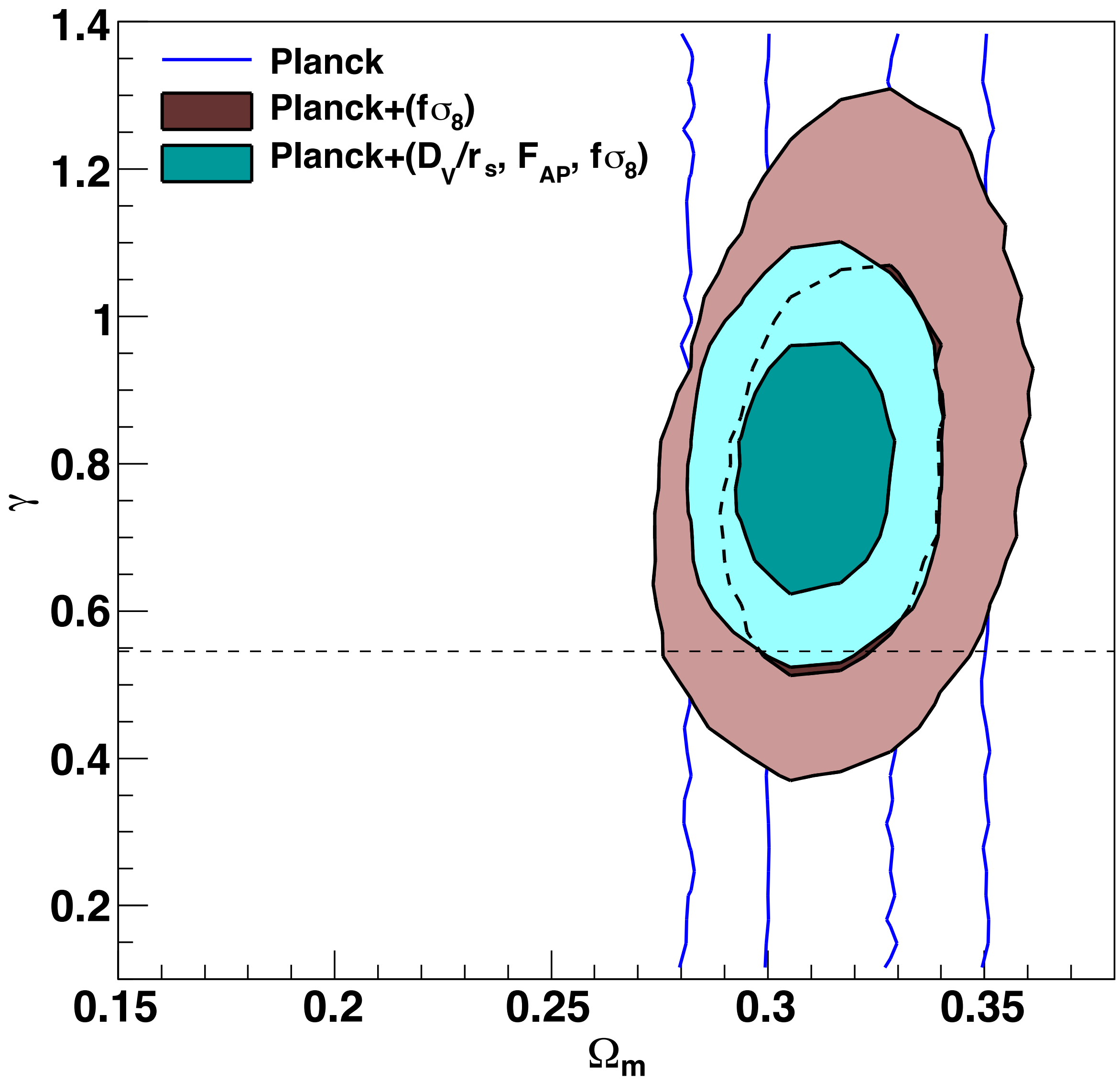

$$f \equiv \frac{d\ln D(a)}{d\ln a} = \Omega_m^{\gamma}(z)$$

Beutler *et al.* (2014)
BOSS collaboration

The future

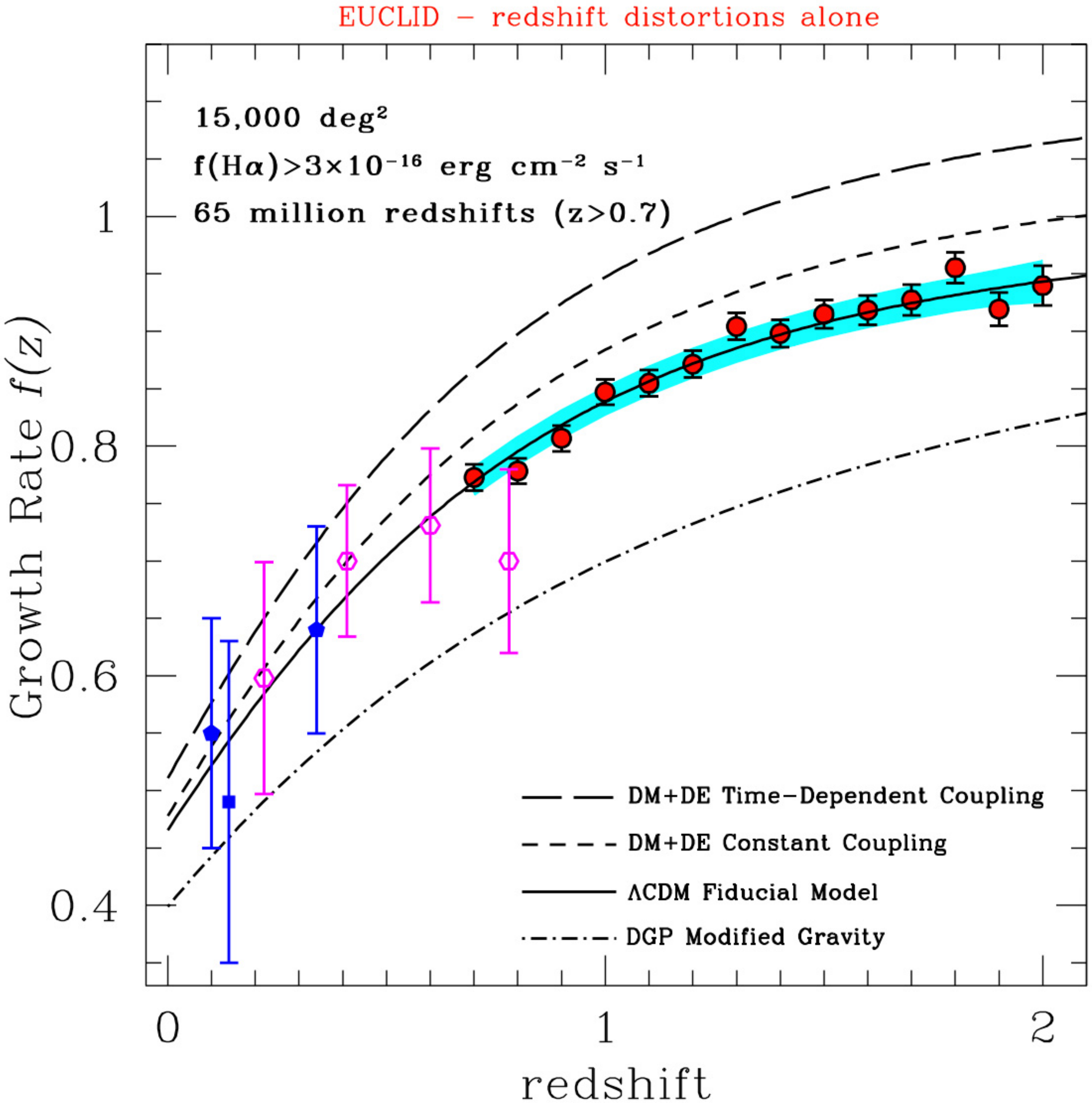

Euclid Theory Group

Neutrinos

Neutrinos in the Universe

Neutrinos in the early Universe (at high temperature) are kept in equilibrium with other species by weak interactions

$$f_{\rm eq}(p) = \left[\exp\left(\frac{p}{T}\right) + 1\right]^{-1}$$

Fermi-Dirac distribution

They decouple when the temperature drops below $T \sim 1\,\mathrm{MeV}$

Therefore they decouple when ultra relativistic!

Two regimes:

- At **high redshift** they (mostly) contribute to the **radiation** energy density
- At **low redshift** they (mostly) contribute to the **matter** energy density

$$1 + z_{nr} \simeq 1890 \frac{m_{\nu,i}}{1\ \mathrm{eV}} \qquad \Omega_{\nu,0} h^2 = \frac{M_\nu}{93.14\,\mathrm{eV}}.$$

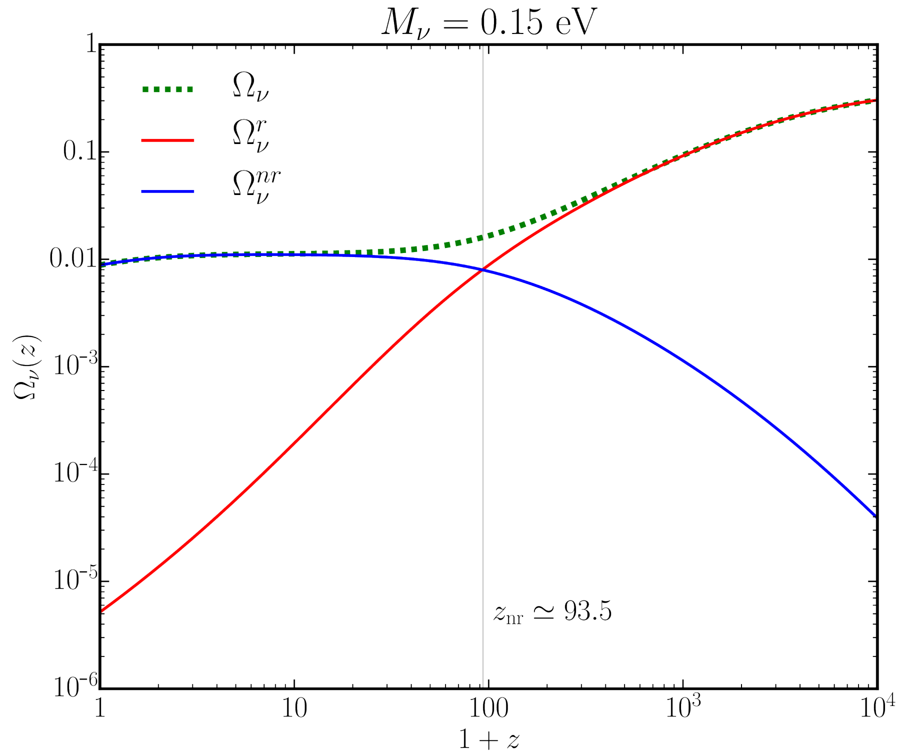

The free-streaming scale

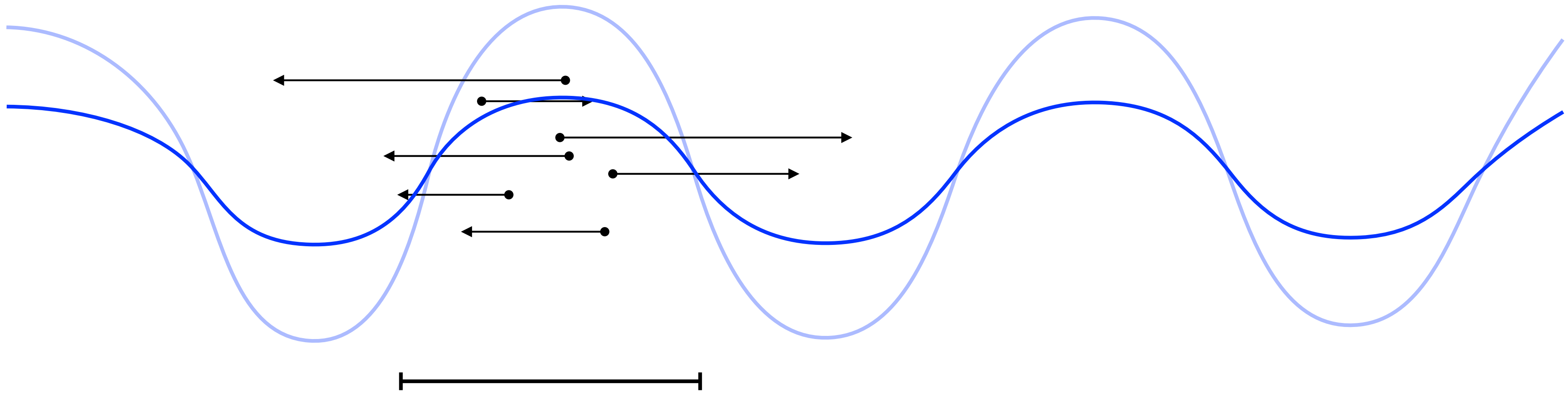

$$\lambda_{\rm FS} \sim 1/k_{\rm FS}$$

$$\sigma^2_{\nu,{\rm i}}(z) \equiv \frac{\int d^3p\, p^2/m^2_{\nu,{\rm i}}(\exp[p/T_\nu(z)]+1)^{-1}}{\int d^3p\, (\exp[p/T_\nu(z)]+1)^{-1}}$$

Velocity dispersion

$$k_{\rm FS,i} \sim \frac{aH(a)}{\sigma_{\nu,i}} \qquad k_{\rm FS,i} \simeq \frac{0.677}{(1+z)^2}\left(\frac{m_{\nu,{\rm i}}}{1\ {\rm eV}}\right)\left[\Omega_m(1+z)^3+\Omega_\Lambda\right]^{\frac{1}{2}}\ h\ {\rm Mpc}^{-1}.$$

$$k_{\rm FS,i} \lesssim 0.1 h{\rm Mpc}^{-1}$$

$$(m_{\nu,i} \lesssim 0.1eV)$$

the free-streaming scale is fairly large (almost linear scales) for viable values of the neutrino mass!

Neutrino clustering

The matter power spectrum

The *total* matter overdensity

$$\delta_m = (1 - f_\nu)\,\delta_c + f_\nu\,\delta_\nu\,,$$

Neutrino fraction:

$$f_\nu \equiv \frac{\Omega_\nu}{\Omega_m} = \frac{\bar\rho_\nu}{\bar\rho_m}$$

The *total* matter power spectrum

$$P_{mm} = (1 - f_\nu)^2\,P_{cc} + 2 f_\nu\,(1 - f_\nu)\,P_{c\nu} + f_\nu^2\,P_{\nu\nu}$$

$$\frac{P_{mm}(k; f_\nu)}{P_{mm}(k; f_\nu = 0)} \simeq 1 - 8 f_\nu$$

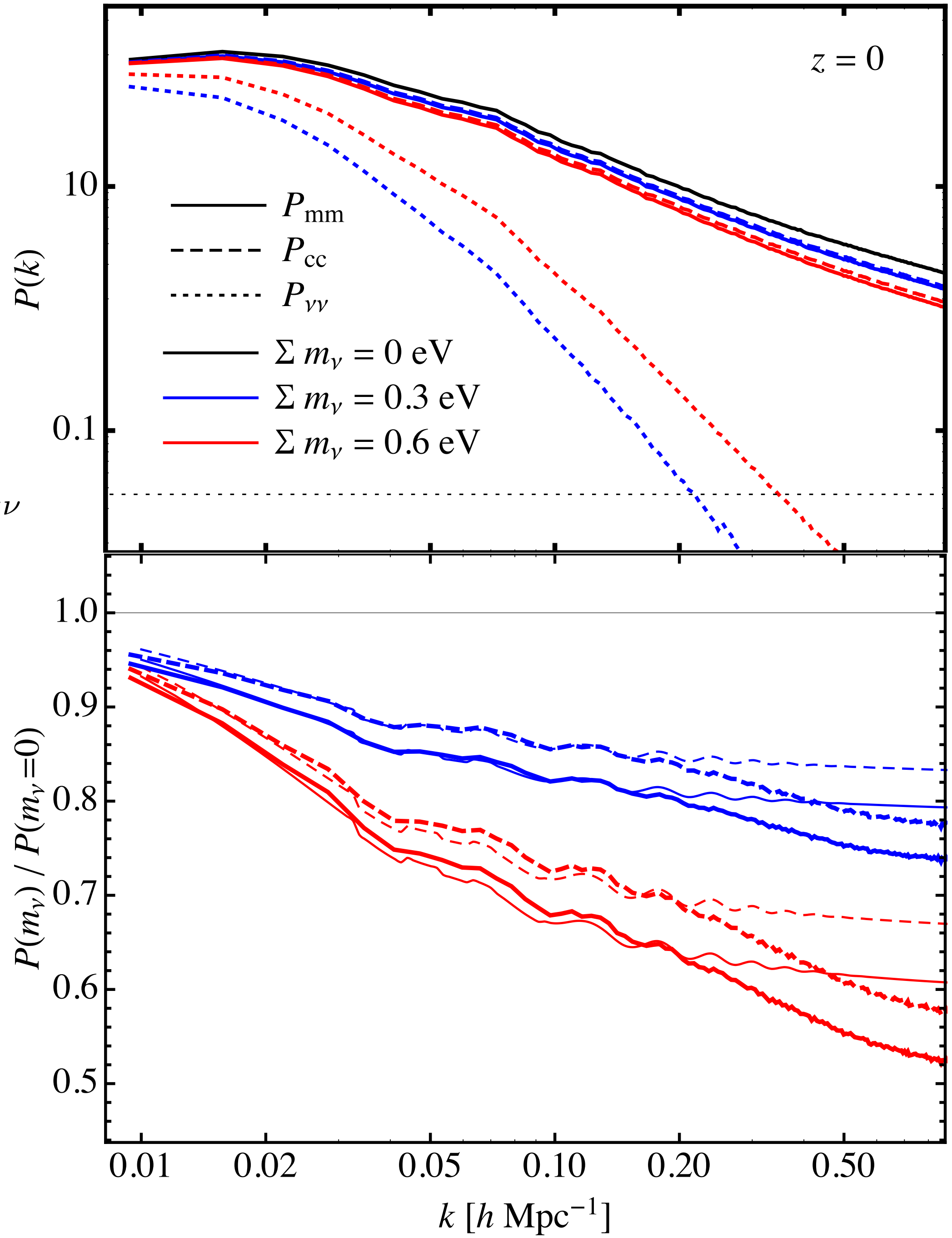

the suppression of the power spectrum due to neutrinos is proportional to the (total) neutrino mass

Constraining neutrino masses

$$\sum m_\nu = 0.36 \pm 0.14 \text{ eV}$$

combined with CMB

LSS could be close to a neutrino mass detection ...

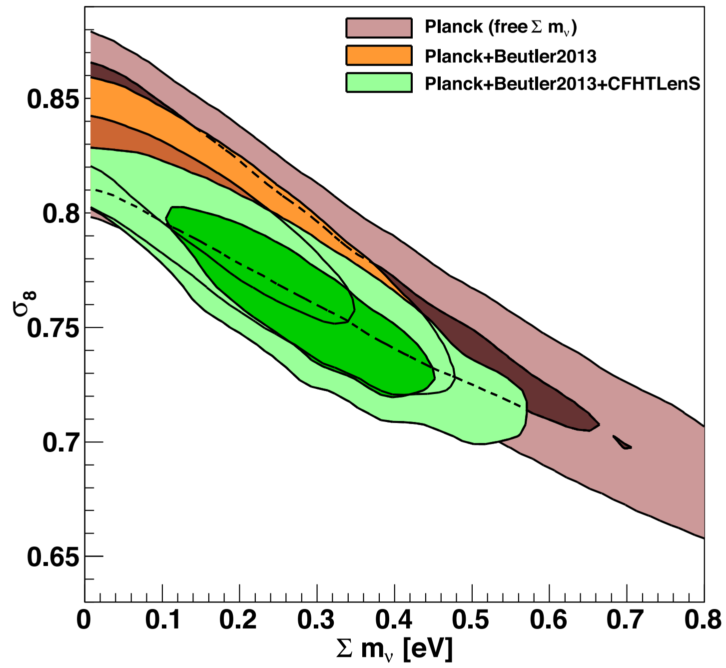

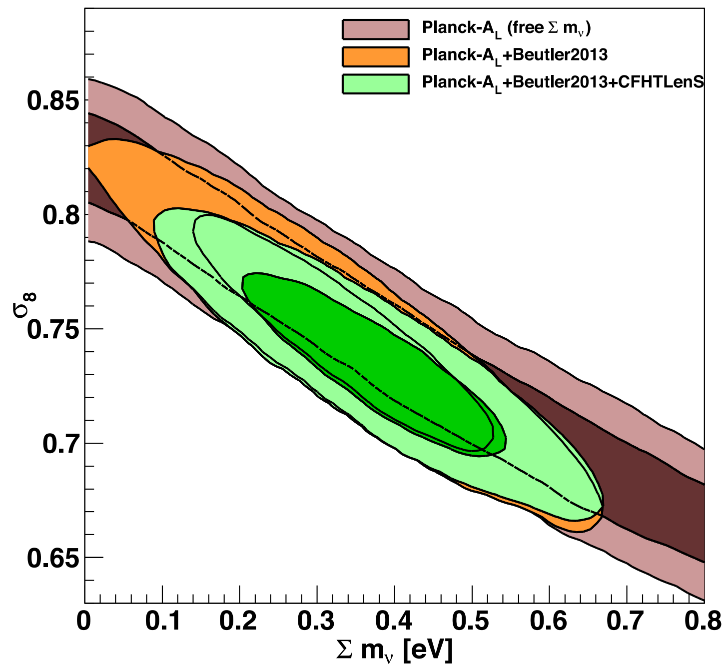

Beutler *et al.* (2014)
BOSS collaboration

Constraining neutrino masses

Data set(s)	σ_8	$\Omega_{\rm m}$	$\sum m_\nu$ (eV) 68 per cent c.l.	$\sum m_\nu$ (eV) 95 per cent c.l.
WMAP9	0.706 ± 0.077	$0.354^{+0.048}_{-0.078}$	<0.75	<1.3
WMAP9+CFHTLenS	$0.696^{+0.094}_{-0.071}$	$0.343^{+0.046}_{-0.078}$	<0.76	<1.3
WMAP9+Beutler2013	0.733 ± 0.038	0.309 ± 0.015	0.36 ± 0.14	0.36 ± 0.28
WMAP9+Beutler2013+CFHTLenS	0.731 ± 0.026	0.308 ± 0.014	0.37 ± 0.12	0.37 ± 0.24
WMAP9+Beutler2013+GGlensing	0.725 ± 0.029	0.307 ± 0.014	0.39 ± 0.12	0.39 ± 0.25
WMAP9+Beutler2013+CFHTLenS+GGlensing+BAO	0.733 ± 0.024	0.303 ± 0.011	0.35 ± 0.10	0.35 ± 0.21
WMAP9+Samushia2013	0.746 ± 0.036	0.303 ± 0.013	0.31 ± 0.13	0.31 ± 0.25
WMAP9+Samushia2013+CFHTLenS+GGlensing+BAO	0.740 ± 0.023	0.2991 ± 0.0097	0.32 ± 0.10	0.32 ± 0.20
WMAP9+Chuang2013	0.717 ± 0.046	0.311 ± 0.015	0.42 ± 0.17	0.42 ± 0.35
WMAP9+Chuang2013+CFHTLenS+GGlensing+BAO	0.728 ± 0.026	0.304 ± 0.011	0.36 ± 0.11	0.36 ± 0.23
WMAP9+Anderson2013	$0.763^{+0.058}_{-0.040}$	0.295 ± 0.011	<0.31	<0.54
WMAP9+Anderson2013+BAO	$0.763^{+0.060}_{-0.041}$	0.2946 ± 0.0093	<0.31	<0.53
WMAP9+Anderson2013+CFHTLenS+GGlensing+BAO	0.750 ± 0.029	0.2936 ± 0.0097	0.27 ± 0.12	0.27 ± 0.22
Planck	$0.775^{+0.074}_{-0.031}$	$0.353^{+0.021}_{-0.058}$	<0.41	<0.95
Planck+CFHTLenS	$0.745^{+0.083}_{-0.112}$	0.332 ± 0.064	<0.51	<1.0
Planck+Beutler2013	$0.791^{+0.034}_{-0.025}$	0.320 ± 0.014	0.20 ± 0.13	<0.40
Planck+Beutler2013+CFHTLenS	$0.760^{+0.026}_{-0.047}$	0.314 ± 0.019	0.29 ± 0.13	$0.29^{+0.29}_{-0.23}$
Planck+Beutler2013+GGlensing	0.769 ± 0.035	0.316 ± 0.016	0.26 ± 0.13	0.26 ± 0.24
Planck+Beutler2013+CFHTLenS+GGlensing+BAO	$0.759^{+0.025}_{-0.033}$	0.306 ± 0.015	0.27 ± 0.12	0.27 ± 0.21
Planck+CMBlensing+Beutler2013+CFHTLenS+GGlensing+BAO	$0.774^{+0.025}_{-0.037}$	0.304 ± 0.014	0.24 ± 0.14	0.24 ± 0.20
Planck+Samushia2013	$0.800^{+0.029}_{-0.023}$	0.315 ± 0.013	$0.161^{+0.068}_{-0.139}$	<0.33
Planck+Samushia2013+CFHTLenS+GGlensing+BAO	0.765 ± 0.031	0.303 ± 0.014	$0.243^{+0.132}_{-0.088}$	0.24 ± 0.19
Planck+Chuang2013	$0.797^{+0.038}_{-0.026}$	0.319 ± 0.014	<0.23	<0.40
Planck+Chuang2013+CFHTLenS+GGlensing+BAO	$0.759^{+0.027}_{-0.037}$	0.306 ± 0.015	0.27 ± 0.12	0.27 ± 0.22
Planck+Anderson2013	$0.821^{+0.023}_{-0.012}$	0.304 ± 0.010	<0.10	<0.22
Planck+Anderson2013+BAO	$0.821^{+0.022}_{-0.013}$	0.3020 ± 0.0084	<0.09	<0.21
Planck+Anderson2013+CFHTLenS+GGlensing+BAO	$0.782^{+0.029}_{-0.048}$	$0.296^{+0.010}_{-0.015}$	0.17 ± 0.12	<0.33
Planck+CMBlensing+Anderson2013+CFHTLenS+GGlensing+BAO	$0.794^{+0.025}_{-0.032}$	0.294 ± 0.012	$0.15^{+0.15}_{-0.12}$	<0.30
Planck+CMBlensing	$0.746^{+0.086}_{-0.038}$	$0.373^{+0.048}_{-0.077}$	<0.62	<1.1
Planck $- A_{\rm L}$	$0.716^{+0.092}_{-0.064}$	$0.356^{+0.043}_{-0.065}$	<0.71	<1.2
Planck $- A_{\rm L}$+CFHTLenS	$0.694^{+0.099}_{-0.079}$	$0.351^{+0.048}_{-0.076}$	$0.62^{+0.36}_{-0.50}$	<1.3
Planck $- A_{\rm L}$+Beutler2013	0.746 ± 0.035	0.316 ± 0.015	0.34 ± 0.14	0.34 ± 0.26
Planck $- A_{\rm L}$+Beutler2013+CFHTLenS	0.733 ± 0.027	$0.314^{+0.013}_{-0.018}$	0.38 ± 0.11	0.38 ± 0.24
Planck $- A_{\rm L}$+Beutler2013+GGlensing	0.733 ± 0.031	$0.314^{+0.013}_{-0.017}$	0.38 ± 0.12	0.38 ± 0.25
Planck $- A_{\rm L}$+Beutler2013+CFHTLenS+GGlensing+BAO	0.736 ± 0.024	0.307 ± 0.011	0.36 ± 0.10	0.36 ± 0.21
Planck $- A_{\rm L}$+CMBlensing+Beutler2013+CFHTLenS+GGlensing+BAO	$0.731^{+0.030}_{-0.040}$	0.309 ± 0.015	$0.38^{+0.12}_{-0.17}$	0.38 ± 0.20
Planck $- A_{\rm L}$+Samushia2013	0.759 ± 0.035	0.310 ± 0.013	0.28 ± 0.12	0.28 ± 0.23
Planck $- A_{\rm L}$+Samushia2013+CFHTLenS+GGlensing+BAO	0.743 ± 0.024	0.303 ± 0.011	0.324 ± 0.099	0.32 ± 0.19
Planck $- A_{\rm L}$+Chuang2013	0.737 ± 0.042	0.318 ± 0.016	$0.38^{+0.15}_{-0.19}$	0.38 ± 0.32
Planck $- A_{\rm L}$+Chuang2013+CFHTLenS+GGlensing+BAO	0.730 ± 0.028	0.309 ± 0.012	0.38 ± 0.11	0.38 ± 0.22
Planck $- A_{\rm L}$+Anderson2013	$0.784^{+0.046}_{-0.026}$	$0.299^{+0.010}_{-0.013}$	<0.23	<0.43

LSS could be close to a neutrino mass detection …

… although we are probably not there yet

Beutler *et al.* (2014)
BOSS collaboration

Constraining neutrino masses & gravity

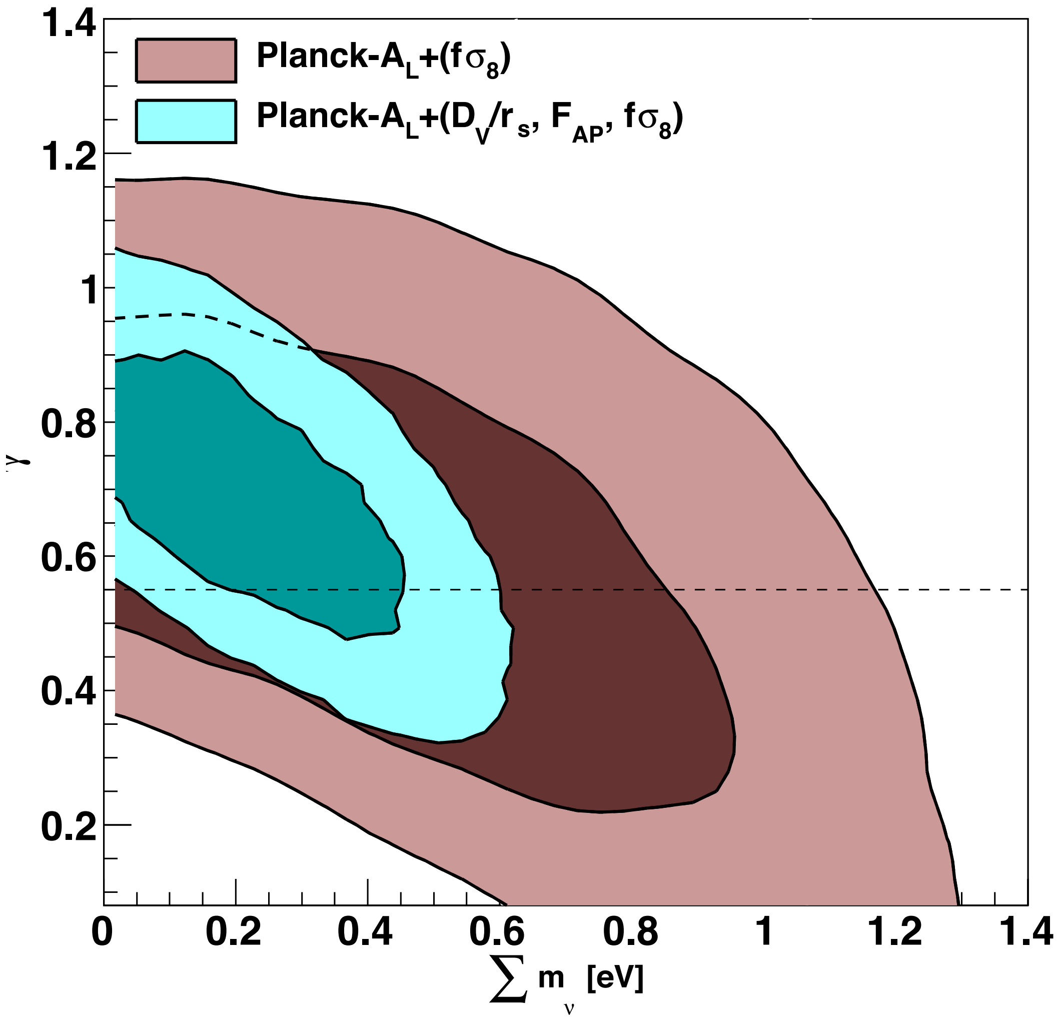

Beutler *et al.* (2014)
BOSS collaboration

Conclusions

Large-scale structure observations

Future galaxy redshift surveys (e.g. DESI from the ground or Euclid from the sky) will continue an on-going effort to map the **large-scale galaxy distribution**

Different **features of the galaxy power spectrum** provide different constraint on the cosmological model:

- **BAO are a *standard ruler*,** a geometrical probe of the expansion history
- The **anisotropy** of the galaxy power spectrum (Redshift-Space Distortions) measure instead the *growth of structure*
- The **"shape" of the power spectrum** provide an upper bound on neutrino masses